Completion of neural crest cell production and emigration is regulated by retinoic acid-dependent inhibition of BMP signaling

Dina Rekler and Chaya Kalcheim,*

Department of Medical Neurobiology, Institute of Medical Research Israel-Canada (IMRIC) and the Edmond and Lily Safra Center for Brain Sciences (ELSC).

Hebrew University of Jerusalem-Hadassah Medical School

Jerusalem 9112102, P.O.Box 12272, Israel

Emails: Dina Rekler, dina.rekler@mail.huji.ac.il; Chaya Kalcheim, kalcheim@cc.huji.ac.il

*To whom correspondence should be addressed.

Running title: Local RA signals the end of neural crest production

Key words: BAMBI, cell specification, dorsal interneurons, Foxd3, Hairy, neural tube, Raldh2, Roof plate, Snai2, Sox9.

Abstract

Production and emigration of neural crest cells is a transient process followed by the emergence of the definitive roof plate. The mechanisms regulating the end of neural crest ontogeny are poorly understood. Whereas early crest development is stimulated by mesoderm-derived retinoic acid, we report that the end of the neural crest period is regulated by retinoic acid synthesized in the dorsal neural tube. Inhibition of retinoic acid signaling in the neural tube prevents the normal upregulation of BMP inhibitors in the nascent roof plate and prolongs the period of BMP responsiveness which otherwise ceases close to roof plate establishment. Consequently, neural crest production and emigration are extended well into the roof plate stage. Although several roof plate-specific genes are normally expressed in the absence of retinoic acid signaling, roof plate and crest markers are co-expressed in single cells and this domain also contains dorsal interneurons. Hence, the cellular and molecular architecture of the roof plate is compromised. Collectively, our results demonstrate that neural tube-derived retinoic acid, via inhibition of BMP signaling, is an essential factor responsible for the end of neural crest generation and the proper segregation of dorsal neural lineages.

Introduction

To ensure normal development, embryogenesis takes place in a stereotypic sequence and a spatially regulated manner. An example of such a precision is the development of the central and peripheral subdivisions of the nervous system (CNS and PNS), that arise from a common domain in the dorsal neural tube (NT). This domain sequentially generates neural crest cells (NC), progenitors of the peripheral nervous system (PNS)(Le Douarin and Kalcheim, 1999), followed by the definitive roof plate (RP) of the CNS, which is flanked ventrally by dorsal interneuron populations (Andrews et al., 2019; Kalcheim and Kumar, 2017; Krispin et al., 2010).

At trunk levels of the avian axis, NC progenitors sequentially emigrate from the NT for a period of about two days while actively proliferating before and after delamination and largely synchronizing to the S-phase of the cell cycle during the emigration event (Burstyn-Cohen and Kalcheim, 2002). Lineage tracing experiments showed that RP progenitors originate ventral to the cohort of premigratory NC (Krispin et al., 2010b). As a result of continuous cell emigration, RP precursors undergo a ventro-dorsal shift and, upon completion of NC departure, they reach the dorsal midline of the NT and form the definitive RP (Krispin et al., 2010b). RP progenitors gradually exit the cell cycle to become post-mitotic (Kahane and Kalcheim, 1998), and function primarily as a dorsal organizer, providing a gradient of Bone Morphogenetic Protein (BMP) and Wnt activity which is crucial for development of dorsal interneurons (Chizhikov and Millen, 2005; Le Dréau and Martí, 2013; Muroyama et al., 2002; Zechner et al., 2007) and for proliferation of ependymal cells at later stages (Shinozuka et al., 2019; Xing et al., 2018).

Many aspects of early NC ontogeny were extensively studied, from induction to specification, epithelial to mesenchymal transition (EMT) and emigration. Yet, virtually nothing is known about the mechanisms underlying the end of NC production and transition to definitive RP (Rekler and Kalcheim, 2021).

57 BMP has been found to regulate several aspects of NC development. In the early neurula, BMP
58 is derived from the non-neural ectoderm and participates in NC induction at the neural plate
59 border (Endo et al., 2003). Upon closure of the NT, cells of the dorsal domain synthesize and
60 secrete BMP, which acts in a graded rostro-caudal fashion to activate Wnt signaling and a
61 network of downstream genes that altogether promote NC EMT and emigration [Reviewed in
62 (Kalcheim, 2018)].

63 A first step towards understanding the segregation between NC and RP, was the finding that
64 approaching the end of the NC production in the avian embryo, the dorsal NT becomes
65 insensitive to BMP, even though this factor continues to be produced by nascent RP cells. This
66 suggested that local downregulation of BMP signaling is necessary for the end of NC stage, a
67 conclusion further illustrated by a premature cessation of NC proliferation and delamination
68 upon early inhibition of BMP signaling (Nitzan et al., 2016). These events were mediated by
69 the transcription factor HES1/Hairy1, as early misexpression of *hes1/hairy1* in the dorsal NT
70 led to a downregulation of the *Alk3* BMP receptor and of pSmad activity (Nitzan et al., 2016).

71 However, the mechanism that orchestrates these BMP-dependent processes, leading to
72 cessation of NC production, segregation of NC and RP lineages, and formation of the definitive
73 RP, remains unknown. Along this line, whether cessation of NC production and RP
74 development are regulated by the same or by independent mechanisms is yet to be elucidated.

75 A recent RNA-seq analysis revealed transcriptional heterogeneity between premigratory NC
76 and definitive RP cells, uncovering a set of genes expressed specifically at the onset of the RP
77 stage (Ofek et al., 2021). One of these genes is *Raldh2/Aldh1a2*, that encodes an enzyme
78 responsible for the biosynthesis of the morphogen retinoic acid (RA) (Haselbeck et al., 1999),
79 central to multiple neurodevelopmental processes (Diez del Corral and Morales, 2014; Lara-
80 Ramírez et al., 2013; Wilson et al., 2004). RA derived from the *Raldh2*-expressing somitic

81 mesoderm has been described as a key factor in NT development, including control of
82 motoneuron specification (Novitch et al., 2003; Wilson et al., 2004) and initiation of NC EMT
83 and emigration (Martinez-Morales et al., 2011). Although expression of *Raldh2* in the dorsal
84 NT was previously reported (Berggren et al., 1999; Blentic et al., 2003), its precise temporal
85 dynamics vis-à-vis NC/RP phases and function/s have not been characterized. Hence, the
86 discovery of local RA production in the dorsal NT only by the end of the NC stage prompted
87 us to hypothesize a role for RA in events concerning the late NC.

88 In this study, we unravel a fundamental role of dorsal NT-derived RA in controlling the end of
89 NC production. Using two separate tools to inhibit RA signaling in the quail embryo, we
90 demonstrate that RA is responsible for downregulation of BMP signaling in the dorsal NT. In
91 the absence of RA signaling, cells in the dorsal NT retain expression of NC markers well into
92 the RP stage which also displays additional NC traits such as a high mitotic rate and impaired
93 epithelial properties. Furthermore, we show that lack of RA signaling prolongs cell
94 delamination into the RP stage. The latter effect is abrogated by concomitant inhibition of BMP
95 signaling, suggesting that, epistatically, RA acts upstream of BMP signaling. Remarkably,
96 maintenance of NC traits in the dorsal NT does not prevent the advent of RP traits, or RP-
97 dependent specification of dorsal interneurons. Rather, in the absence of RA activity, the spatial
98 and temporal segregation of dorsal lineages, as well as the structural integrity of this signaling
99 center, are compromised.

100

101

102

Results

RA is both produced and active in the nascent RP

The spatio-temporal dynamics of RA, including synthesis, degradation and activity, was examined in the trunk of quail embryos from stages corresponding to NC production until formation of the nascent RP. RA is produced from retinol via two consecutive reactions: first, retinol is converted to retinaldehyde by RDH enzymes, then it is oxidized to RA by RALDH/ALDH1; additionally, CYP1B1 catalyzes both reactions [Fig. 1A and (Chambers et al., 2007; Kam et al., 2012; Reijntjes et al., 2005; Rhinn and Dollé, 2012). Of the three known RALDH-encoding genes, only *Raldh2* is expressed in the avian trunk at these developmental stages (Blentic et al., 2003). At an early NC stage, *Raldh2* was expressed in the intermediate and paraxial somitic mesoderm but not in the neuroepithelium (Fig. 1B). At an advanced NC stage, *Raldh2* continued to be transcribed in subdomains of the somite-derived sclerotome and dermomyotome (Fig. 1C) and was weakly detected in the dorsal NT (Fig. 1C, arrowhead). Subsequently, *Raldh2* was strongly expressed in the nascent RP itself (Fig. 1D, arrowhead). In contrast, no expression of *Cyp1B1* was apparent in the NT at any stage, although robust transcription was evident in the paraxial mesoderm throughout development (Fig. 1E-G).

RA is degraded by CYP26 enzymes of the cytochrome P450 family. *Cyp26A1* is the only member of the family to be expressed in the avian trunk at early stages of nervous system development (Blentic et al., 2003). At an early NC stage, *Cyp26A1* was absent from the NT and adjacent mesoderm, it was later detected in a salt and pepper pattern in dorsal interneuron progenitors, but was excluded from the dorsal midline (Fig. 1H-I). As the definitive RP formed, it was also occasionally detected in RP cells (Fig. 1J).

CRABP-I is a carrier protein of RA, which participates in regulation of RA function and/or metabolism (Maden et al., 1989; Venepally et al., 1996). At the early NC stage there was no

127 prominent expression of *CrabpI* in either the NT or paraxial mesoderm (Fig. 1K); at an
128 advanced NC stage it appeared in the basal domain of the NT, corresponding to the positions
129 adopted by differentiating neurons, yet absent from the dorsal and ventral midline regions (Fig.
130 1L). At the RP stage *CrabpI* was additionally expressed in two stripes at the lateral domain of
131 the RP [(Fig. 1M, and see (Ofek et al., 2021)].

132 Next, we examined expression of RA receptors. RA acts by binding to a heterodimer of nuclear
133 receptors, RAR and RXR, each of which is encoded by three genetic variants. Expression of
134 all RA receptors was predominantly ubiquitous with at least one variant of each subunit
135 expressed in the dorsal NT at both NC and RP stages (RARα, RARβ and RXRγ, respectively,
136 but not RARγ or RXRα) (Supplem. Fig. S1). The dynamic expression of various components
137 of the RA pathway, suggests that RA acts not only during early NC development, but also
138 during the transition into the nascent RP where a tight regulation of local RA levels may take
139 place.

140 To directly examine the activity of RA in the dorsal NT, we electroporated a distable GFP
141 plasmid driven by a retinoic acid response element (RARE-d2EGFP) at E2.5 and analyzed GFP
142 fluorescence 12 and 48 hours later, at NC and RP stages, respectively. Whereas control RFP
143 was apparent throughout the dorso-ventral extent of the NTs, RARE activity was primarily
144 present within the dorsal half of the NT at both stages (Fig. 1N-O').

145 Together, these data show that whereas NC cells respond to mesoderm-derived RA (see
146 Introduction for refs.), but do not synthesize it, the emerging RP both synthesizes and responds
147 to this factor. Hence during the transition from NC to definitive RP, the latter becomes a local
148 source of RA. This prompted us to hypothesize that locally produced RA plays a role in either
149 the end of NC production and emigration, in the ensuing formation of the RP, or in both
150 processes.

151

Figure 1

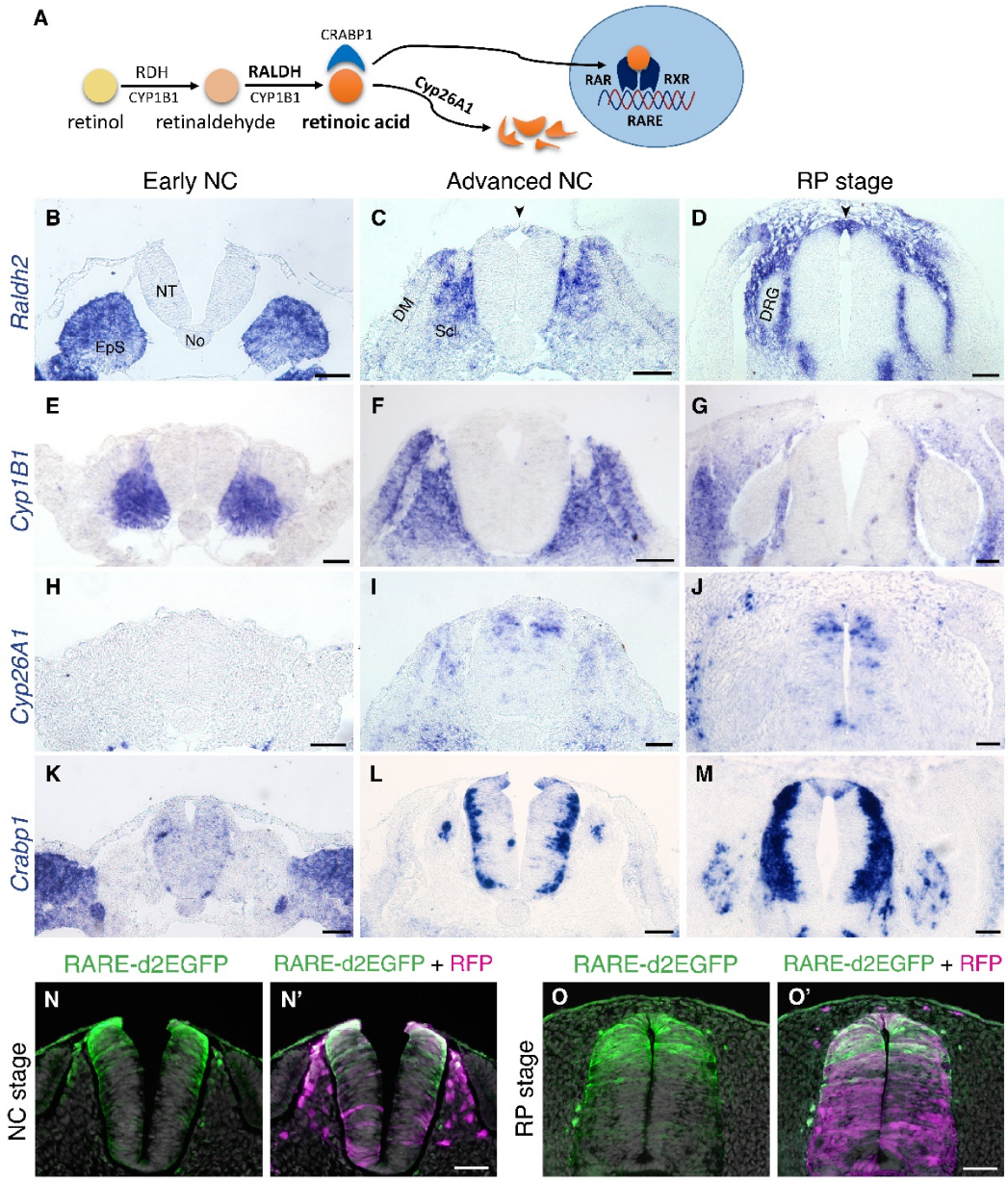

Figure 1- RA is both produced and active in the nascent RP

(A) Schematic illustration of the metabolic and signaling pathways of RA.

(B-M) Expression patterns of genes participating in RA synthesis and metabolism, both at early and advanced NC stages (E2 and E3, respectively), and at the RP stage (E4). ISH for *Raldh2/Aldh1a2* (B-D), *Cyp1B1* (E-G), *Cyp26A1* (H-J) and *Crabp1* (K-M).

(N-O') RA activity in the NT at NC and RP stages, indicated by the presence of distable GFP (d2EGFP) driven under the control of a RARE element. Embryos were electroporated at E2.5 along with control RFP to monitor efficiency of transfection, and analyzed 12 hours (N-N') or 48 hours (O-O') later. RARE activity was evident in the dorsal NT of NC-stage embryos (N=8/8), and RP-stage embryos (N=7/7).

Abbreviations, EpS, epithelial somite, No, notochord, NT, neural tube, DM, dermomyotome, Scl, sclerotome, DRG, dorsal root ganglion. Scale bar, 50 µm.

165 **RA is responsible for the loss of sensitivity of dorsal NT progenitors to BMP during the**
166 **transition from NC to RP**

167 In previous studies, we showed that BMP signaling is essential for NC EMT and emigration
168 (Sela-Donenfeld and Kalcheim, 1999). Subsequently, when approaching the RP stage,
169 although BMP is still produced by the nascent RP, the latter becomes refractory to it, likely
170 via downregulation of BMP receptor 1A (*Alk3*), and upregulation of BMP inhibitory genes
171 (Nitzan et al., 2016; Ofek et al., 2021). The onset of *Raldh2* synthesis close to RP development
172 prompted us to hypothesize that RA, locally produced in the dorsal NT, regulates this dynamic
173 cellular behavior vis-a-vis BMP. To this end, we implemented two independent means to
174 inhibit RA activity *in vivo*: 1) RARα403 - a truncated human RA receptor that lacks the
175 transactivation domain and therefore acts in a dominant-negative fashion (Gupta and Sen,
176 2015) , and 2) Cyp26A1 which encodes a RA-degrading enzyme.

177 First, the efficacy of these constructs was tested by co-electroporation with RARE-RFP. RFP
178 intensity was significantly reduced by 79% and 88% in Cyp26A1- and RARα403-
179 electroporated embryos, respectively, when compared to GFP-only controls. Similarly,
180 RARα403 almost completely abolished the RARE-AP signal observed in controls (Supplem.
181 Fig. S2). Thus, both RARα403 and Cyp26A1 can be effectively used to examine the
182 consequences of RA signaling inhibition.

183 Next, we investigated the effect of RA on the dynamics of BMP signaling. NTs were
184 electroporated at E2.5 (25-27 somite pairs at the level of epithelial somites, NC stage) with
185 either RARα403 or Cyp26A1 and analyzed 2 days later (E4, RP stage) for pSmad1/5/8
186 expression, a readout of BMP activity. As expected (Nitzan et al., 2016), the RP of control
187 embryos was already devoid of BMP activity at this stage (Fig.2A,A', arrows). In contrast, the
188 RP domain of embryos treated with either RARα403 or Cyp26A1 was pSmad-positive,

189 indicating a failure to normally downregulate BMP signaling (Fig. 2B-C', arrowheads). The
190 dI1 progenitor population of dorsal interneurons, located ventral to the RP, was also pSmad-
191 positive, consistent with its dependency on BMP for proper development (Duval et al., 2019;
192 Lee et al., 1998; Tozer et al., 2013; Wine-Lee et al., 2004). Quantification of pSmad intensity
193 confirmed a significant increase in Cyp26A1 and RARα403-treated embryos compared to
194 controls. This was apparent even if measurement of pSmad intensity comprised the dorsal NT
195 from its midline to the ventral border of pSmad+ staining, that included dI1 progenitors (Fig.
196 2D). These results show that endogenous RA activity accounts for the downregulation of BMP
197 signaling in the dorsal NT during the transition from NC to RP.

198 We next examined whether the observed RA-dependent downregulation of BMP activity is
199 mediated by a corresponding upregulation of BMP inhibitors at the RP stage. In this context,
200 Hairy1 was previously reported to act as a specific RP-derived BMP inhibitor thus participating
201 in the end of NC production (Nitzan et al., 2016). Furthermore *hairy1/qHes4*, and the known
202 BMP inhibitors *BAMBI* (Brazil et al., 2015) and *Grem1* (Sun et al., 2006), were unraveled as
203 specific RP markers in a recent RNA-seq analysis comparing dorsal NT cells at both
204 premigratory NC and RP stages (Ofek et al., 2021). Embryos electroporated with either
205 Cyp26A1 or RARα403 at E2.5 exhibited a substantially decreased intensity of *BAMBI* mRNA
206 staining in the RP relative to controls (Fig. 2E-H). Similarly, RARα403 significantly affected
207 the upregulation of both *hairy1* and *Gem1* in RP when compared to control embryos (Fig. 2I-
208 N). These results show that the downregulation of BMP signaling by RA is accounted for, at
209 least partially, by upregulation of BMP inhibitory genes.

210 In a previous study, we reported that BMP-dependent emigration of NC cells is mediated by
211 Wnt activity (Burstyn-Cohen et al., 2004), raising the possibility that, in the absence of RA,
212 enhanced Wnt activity is associated with extended BMP signaling at the RP stage. To this end,

213 we assessed the effect of RA inhibition on Wnt signaling in RP by electroporating a distable
214 Wnt reporter, 12XTopFlashd2GFP, together with control RFP or RARα403/RFP. Whereas
215 very low 12XTopFlashd2GFP expression was apparent under control conditions, significantly
216 enhanced expression in the RP was monitored in the RARα403-transfected NTs (Supplem.
217 Fig. S3). Together, these results suggest an involvement of RA activity in the downregulation
218 of BMP and of downstream Wnt signaling towards ending NC production and/or emigration.

Figure 2

Figure 2- RA is responsible for the loss of sensitivity of dorsal NT progenitors to BMP during the transition from NC to RP.

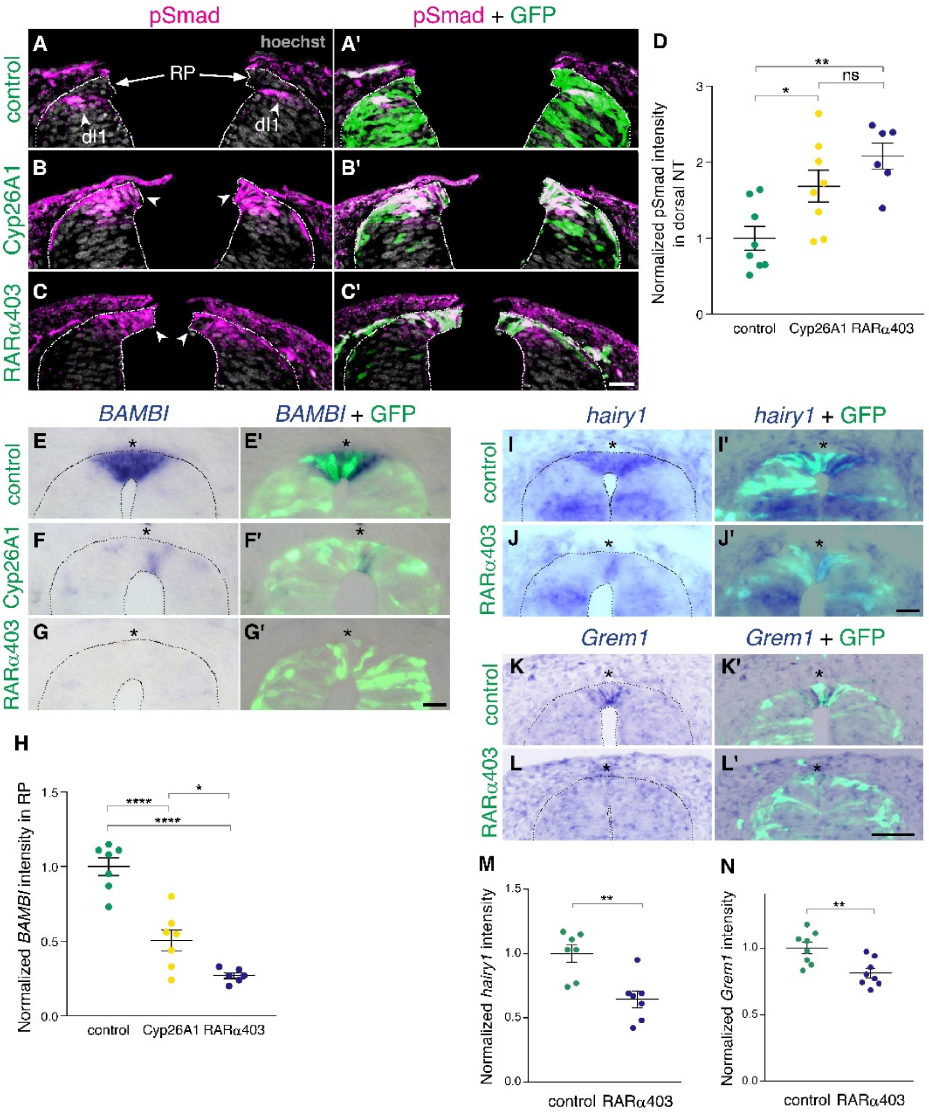

(A-C') Immunostaining for pSmad1/5/8. Embryos at E2.5 were co-electroporated with RARα403, Cyp26A1 or with a control PCAGG vector, along with GFP, and analyzed at E4. Note absence of BMP activity in the RP of control embryos (N=8, A-A') whereas only ventrally located dorsal interneurons are positive, while the RP domain itself is positive in Cyp26A1 (N=8) and RARα403-electroporated embryos (N=7, B-B',C-C'). (D) Quantification of pSmad staining intensity (measured area includes dorsal interneurons). Four-to-21 sections per embryo were analyzed. *p < 0.05, **p < 0.005 , one-way ANOVA with post-hoc Tukey's tests.

(E-N) In-situ hybridization of embryos electroporated with Cyp26a1 or RARα403 at E2.5 and analyzed at E4. Asterisks mark the RP domain.

(E-H) ISH for *BAMBI*, showing downregulation in the RP of Cyp26A1- and RARα403-treated embryos. (H) For quantification of the intensity of *BAMBI*, 6-to-21 sections per embryo were analyzed. N = 7,7 and 6 embryos for control, Cyp26A1 and RARα403, respectively. *p < 0.05, ****p < 0.0001, one-way ANOVA with post-hoc Tukey's tests.

(I-J, M) ISH for *hairy1*, showing downregulation in the RP of RARα403-treated embryos. (M) For quantification of the intensity of *hairy1,* 7-18 sections per embryo were analyzed. N = 7 embryos for each group. **p < 0.005, Student's unpaired t-test.

(K-L,N) ISH for *Grem1*, showing downregulation in the RP of RARα403-treated embryos. For quantification of the intensity of *Grem1*, 11-27 sections per embryo were analyzed. N= 8 embryos for each group. **p < 0.005 via Student's unpaired t-test. Abbreviations, dI1, dorsal interneurons 1, RP, roof plate. Scale bar, 50 µm.

259 **RA downregulates NC markers during the transition to definitive RP**

260 Our results prompted us to investigate whether the observed persistence of BMP and Wnt
261 activity into the RP stage is associated with a retention of NC identity.

262 *Foxd3*, *snai2* and *sox9* are known premigratory markers of trunk NC cells (Nieto et al., 1994;
263 Sela-Donenfeld and Kalcheim, 1999), and are downregulated in the dorsal NT upon emigration
264 of neural progenitors, being absent from prospective melanoblasts and RP (Krispin et al.,
265 2010b; Nitzan et al., 2012; Ofek et al., 2021). Expression of *foxd3*, *snai2* and *sox9* transcripts
266 was examined at the RP stage in embryos electroporated with RARα403. Strikingly, whereas
267 no mRNA expression was detected in controls, all three genes persisted in the dorsal NT of
268 treated embryos (Fig. 3A-F', arrowheads). Moreover, using immunohistochemistry to assess
269 Sox9 protein, we confirmed its maintenance in the dorsal NT at the RP stage both in Cyp26A1-
270 and RARα403-electroporated embryos (Fig. 3G-J).

271 These findings suggest that endogenous RA signaling underlies the loss of NC identity towards
272 the end of the NC period.

273

Figure 3

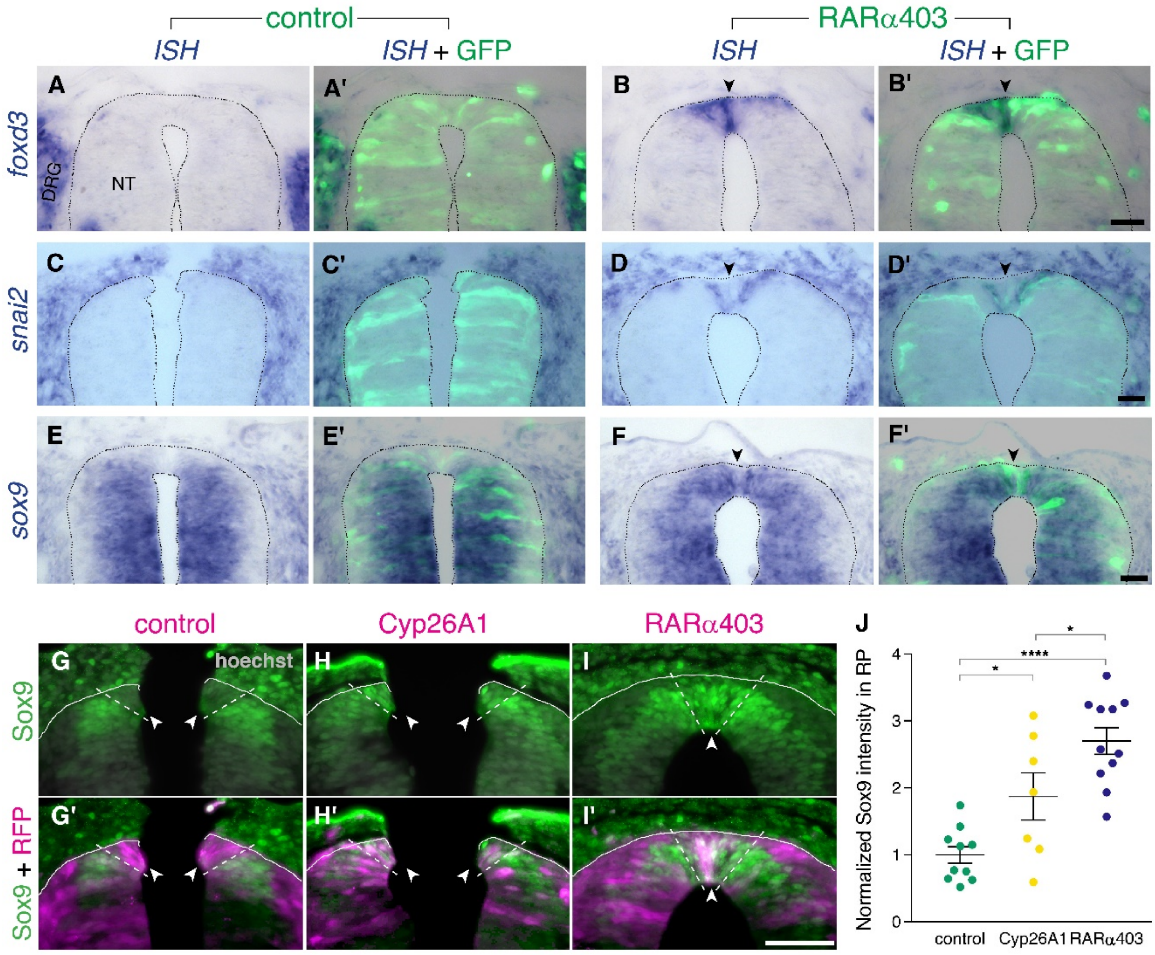

Figure 3- RA downregulates NC markers during the transition to definitive RP

(A-F') ISH for neural crest markers on embryos electroporated with GFP along with control PCAGG or RARα403 at E2.5 and analyzed at E4. Arrowheads point to the RP in RARα403-treated embryos. (A-B') ISH for *foxd3*, showing no expression in the RP of control embryos (N= 7) compared to strong expression in the RP of all RARα403-treated embryos (N = 7). (C-D') ISH for *snai2*, showing no expression in the RP of control embryos (N = 11) and clear expression in the RP of all RARα403-treated embryos (N = 11). (E-F) ISH for *sox9*, showing no expression in the RP of control embryos (N = 9) and strong expression in the RP of all RARα403-treated embryos (N = 9). Note as well expression of *sox9* mRNA in more ventral regions of the NT and in adjacent sclerotome.

(G-J) Immunostaining for Sox9 in control and experimental embryos, showing the presence of Sox9 protein in the RP of Cyp26A1- and RARα403-treated embryos (arrowheads), compared to absence of Sox9 in the RP of control embryos. RFP was co-electroporated in both groups. Dashed lines delineate the RP domain. (J) Measurement of Sox9 staining intensity. For quantification, 15 sections per embryo were analyzed. N = 10, 7, and 11 embryos for control, Cyp26A1 and RARα403 groups, respectively. *$p < 0.05$, ****$p < 0.0001$, one-way ANOVA with post-hoc Tukey's tests. Abbreviations, NT, neural tube, DRG, dorsal root ganglion. Scale bar, 50 μm.

293 **RA signaling promotes cell cycle exit and epithelial traits in dorsal NT cells**

294 NC cells proliferate extensively while residing in the NT and also during migration. Upon the
295 end of NC production, dorsal NT progenitors gradually exit from the cell cycle to become post-
296 mitotic RP cells (Kahane and Kalcheim, 1998; Nitzan et al., 2016). We asked whether RA
297 inhibition affects cell cycle withdrawal of nascent RP cells. To this end, we immunostained
298 embryos at E4 (RP stage) for the mitotic marker phosphohistone H3 (pH3), following
299 electroporation of RARα403 or Cyp26A1 at E2.5 (NC stage). Remarkably, a significantly
300 higher number of mitotic nuclei was observed in the RP of embryos treated with either
301 Cyp26A1 or RARα403 compared to controls which exhibited a low extent of mitosis (Fig. 4A-
302 D). These results suggest that endogenous RA inhibits cell proliferation, consistent with
303 previous data obtained in forebrain and optic tectum of avian embryos (Gupta and Sen, 2015;
304 Kukreja et al., 2020).

305 Furthermore, characteristic of post-mitotic, differentiating progenitors is the localization of
306 nuclei to the basal domain of the neuroepithelium, as observed in control embryos at the RP
307 stage (Fig. 4E). In contrast, in RARα403-electroporated embryos, nuclei were spread
308 throughout its apico-basal extent. Quantification showed that their localization to the apical
309 half of the epithelium significantly exceeds that seen in control conditions (Fig. 4E-G). This is
310 consistent with the higher extent of cell proliferation monitored in the absence of local RA
311 signaling, reflecting the retention of interkinetic nuclear migration with presence of mitotic
312 nuclei in the ventricular zone, and/or a disorganization of the nascent RP under experimental
313 conditions.

314 Another critical process that occurs following the end of NC emigration is the restoration of
315 epithelial cell traits in the nascent RP (Nitzan et al., 2016). One of these traits is the deposition
316 of a continuous and prominent laminin-containing basal lamina covering the normal RP (Fig.

317 4H,H'). This basal lamina is incomplete at the NC stage due to continuous cell delamination.
318 Inhibition of RA signaling resulted in a weaker and discontinuous pattern of laminin
319 immunostaining dorsal to the RP (Fig. 4I-J), indicative of the maintenance of NC
320 characteristics at the later RP stage. Consistently, upon electroporation with membrane-
321 tethered GFP, it was apparent in controls that cells extended along the apico-basal domain of
322 the RP (Fig. 4H). In contrast, in the absence of RA activity, many cells were devoid of epithelial
323 integrity, including labeled cells detaching from the epithelium (Fig.4I, arrows). Combined,
324 these results show that inhibition of RA signaling in the dorsal NT prevents cells from exiting
325 the cell cycle and from adopting cellular traits that characterize the normal ontogeny of a RP.

Figure 4

Figure 4- RA signaling promotes cell cycle exit and epithelial traits in dorsal NT cells

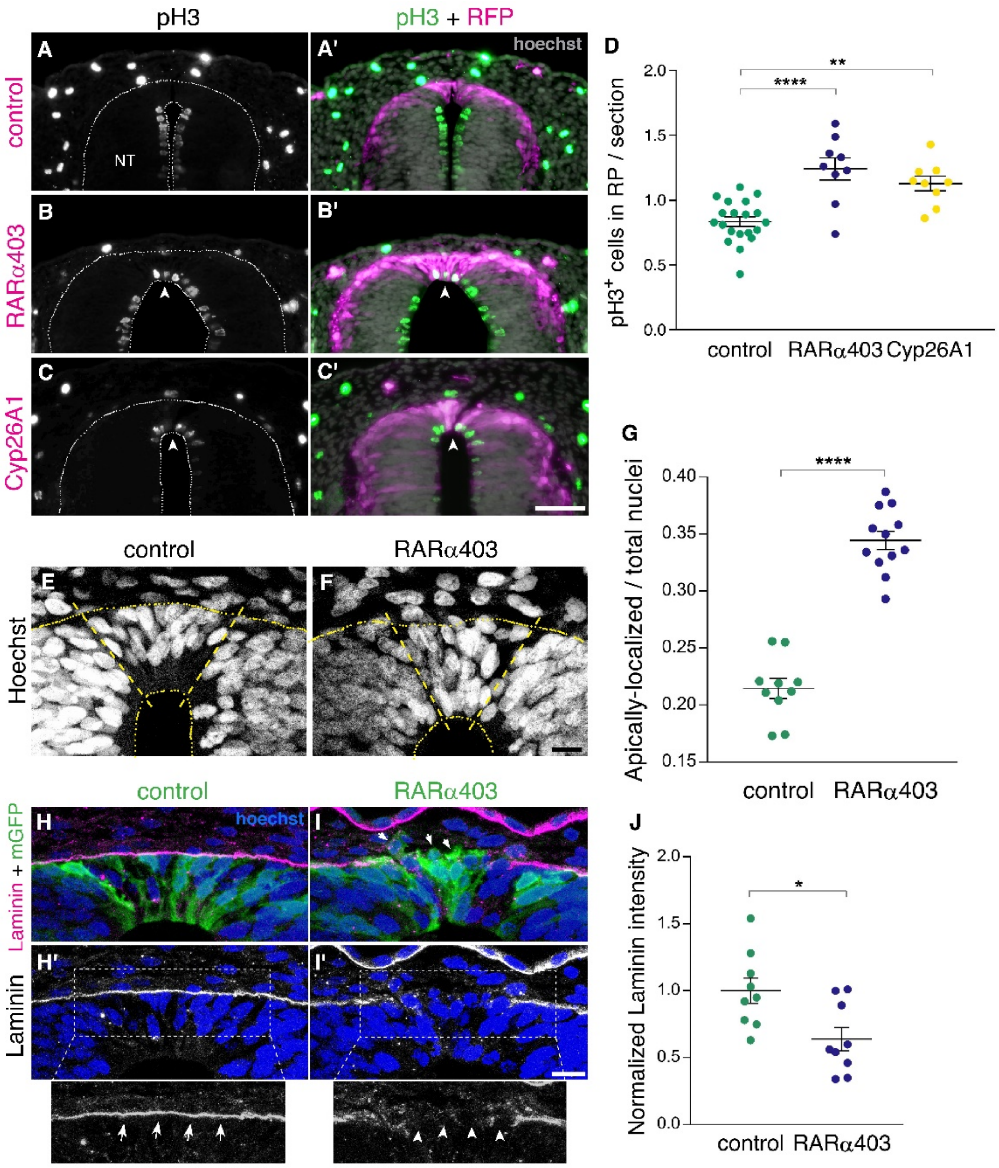

(A-D) Immunostaining for phospho-Histone H3 of embryos electroporated at E2.5 with either control PCAGG, RARα403 or Cyp26A1, and analyzed at E4. Arrowheads in B-C' point to pH3$^+$ cells in the RP domain of RARα403- and Cyp26A1-electroporated embryos. The quantification of pH3$^+$ cells in the RP is represented in (D). 120 sections were analyzed per embryo. N = 20, 9 and 9 embryos for control, RARα403 and Cyp26A1, respectively. **p < 0.005, ****p < 0.0001, one-way ANOVA with post-hoc Tukey's tests.

(E-G) Apico-basal localization of Hoechst-stained nuclei in embryos electroporated as in A-D. Whereas in control embryos most nuclei are restricted to the basal domain of the RP, in the RP of RARα403-treated embryos, nuclei are apparent across the entire thickness of the tissue. Confocal images were z-stacked and nuclei in the apical and basal halves of the RP domain were counted. The proportion of apically-localized nuclei is represented in (G). Thirteen-to-17 sections were analyzed per embryo. N = 10 and 12 embryos for control and RARα403 groups, respectively, ****p < 0.0001, exact p-value Mann-Whitney test.

(H-J) Immunostaining for Laminin of embryos electroporated as in A-D. Arrows and arrowheads in insets of H' and I' indicate the presence of either a continuous or a discontinuous RP basal lamina, respectively. Arrows in I point to delaminating cells. (J) Quantification of Laminin intensity along the basal aspect of the RP. Six-to-18 sections were analyzed per embryo. N = 9 embryos both for control and RARα403 treatments. *p < 0.05, Student's unpaired t-test. Abbreviations, NT, neural tube. Scale bar, (A-C), 50 µm, (E-F, H-I), 10 µm.

367 **RA is responsible for the end of NC delamination**

368 As described above, inhibiting RA activity in the dorsal NT extends the period of BMP activity
369 and preserves NC properties such as premigratory genes and cell proliferation into the RP stage.
370 We therefore asked whether the most discernible difference between NC cells and definitive
371 RP cells, the process of EMT and cell delamination, is prolonged as well by manipulation of
372 RA signaling.

373 To this end, we implemented a double electroporation protocol: first, we electroporated
374 RARα403 along with RFP only to one hemi-NT at E2 and at E3.5 both sides were labeled with
375 GFP-DNA (Fig.5A). By E4, RFP-positive NC cells exited the NTs under both control and
376 treated conditions primarily towards the side ipsilateral to the transfection and also to some
377 extent towards the contralateral side, as previously described (Burstyn-Cohen and Kalcheim,
378 2002; George et al., 2007). However, the number of emigrated, late GFP-labeled cells was
379 significantly higher on the RARα403-electroporated side when compared to the control
380 contralateral side and also to both sides of control embryos (Fig. 5B-D, arrowheads in C').
381 These data show that RA signaling promotes the end of NC cell delamination.

382 Next, we examined the relationship between RA and BMP activities in the context of NC EMT.
383 We hypothesized that, if the end of NC EMT is mediated by RA-dependent inhibition of BMP
384 signaling, the continuous NC emigration observed at the RP stage in response to RARα403,
385 should be prevented by inhibiting BMP with Smad6 (Nitzan et al., 2016).

386 Embryos aged E2 were bilaterally electroporated (Fig. 5A, bottom) with either control GFP,
387 RARα403 to induce late NC delamination (Fig. 5B-D), with Smad6, or with both RARα403
388 and Smad6. At E3.5, control GFP was bilaterally delivered to all embryos and the outcome was
389 analyzed at E4 (Fig. 5A). In all cases, RFP-labeled cells that indicate the efficiency of early
390 transfections, successfully delaminated from the NT. In contrast, under control conditions, few

391 or no GFP-labeled cells delaminated from the NT (Fig.5E-E',I), consistent with the second
392 electroporation being done following the end of NC emigration. As also shown above, in
393 RARα403-treated embryos, a substantial number of GFP-labeled cells had emigrated (Fig. 5F-
394 F',I and see also D). Treatment with Smad6 alone resembled the control situation with few
395 delaminated GFP+ cells at the RP stage (Fig. 5G-G',I), and this effect was not different upon
396 co-transfection of Smad6 and RARα403 (Fig. 5H-H',I). Together, these results show that RA
397 acts upstream of BMP.

398 Next, we examined whether the late-delaminating cells exhibit a NC identity. For this purpose,
399 embryos double electroporated as described in Fig 5A were immunostained for the NC marker
400 HNK1. While in control embryos no GFP-labeled cells were apparent outside the NT, and
401 HNK1 stained only NC derivatives such as dorsal ganglia and ventral roots, in RARα403-
402 treated embryos a considerable number of GFP+HNK1+ cells was also detected in the
403 mesenchyme near the NT (Supplem. Fig. S4A-B", arrowheads in B-B"). Remarkably, 95 ±
404 0.8% of the late-delaminating GFP-labeled cells were $HNK1^{+}$ (Fig. S4C), confirming their NC
405 nature.

406 In addition, we examined the pattern of *foxd3*, which is expressed both in premigratory and
407 migrating NC cells. Embryos were electroporated with RARα403 along with GFP at E2.5 and
408 analyzed at E4. Control NTs were devoid of *foxd3* mRNA in the RP and mRNA signal was
409 only detected in NC derivatives and dI2/V1 interneurons. In RARα403-treated embryos *foxd3*
410 expression was evident in the dorsal NT (see also Fig. 3), and also in NC cells that presumably
411 emigrated recently (Fig S4D-E', arrowheads), further confirming their NC identity.

412 Thus, local RA inhibition in the NT extends the period of NC production and further
413 delamination into the RP stage. Collectively, these results point to RA being a major regulator
414 of the end of the NC stage.

Figure 5

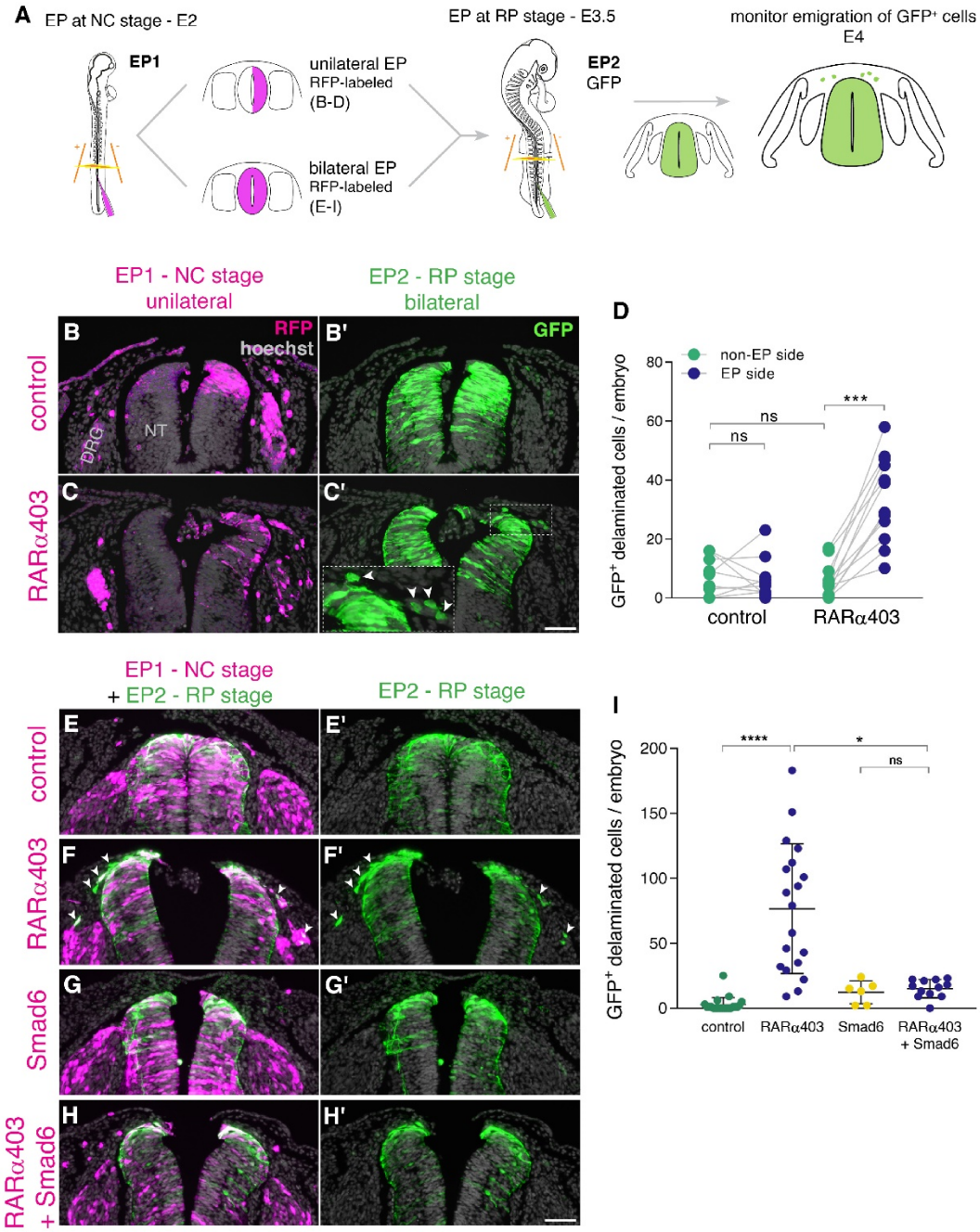

415

416 Figure 5- RA is responsible for the end of NC delamination

417 (A)Schematic representation of the experimental design for detection of late-emigrating cells
418 (see text for details). (B-D) Embryos electroporated unilaterally at E2 with either control or
419 RARα403 plasmids, followed by a second bilateral electroporation at E3.5 with control GFP.
420 Emigration of GFP$^+$ cells was compared between electroporated and non-electroporated sides
421 of control and experimental embryos (D). RFP was delivered with the early electroporation to
422 monitor transfection efficiency. Images presented are adjacent to the rostral somitic domain.
423 Whereas few GFP$^+$ cells delaminated at the RP stage in controls, C' and inset show late-
424 delaminating GFP$^+$ cells ipsilateral to the early RARα403 electroporation (arrowheads). (D)
425 Quantification of GFP$^+$ cells that emigrated from either intact or electroporated (EP) sides of
426 control and experimental embryos. Seventy two sections per embryo were analyzed at an

427 equivalent axial level. N = 10 and 11 embryos for control and RARα403 groups, respectively.
428 Statistical tests applied were exact P-value Wilcoxon signed ranks paired test to compare
429 between EP and non-EP sides of embryos inside each experimental group, and exact P-value
430 Mann-Whitney test to compare between non-EP sides of control and RARα403 groups. ***p
431 < 0.001.

432 (E-I) Embryos were electroporated bilaterally at E2 with control, RARα403, Smad6 or
433 RARα403+Smad6 constructs along with RFP. At E3.5, bilateral electroporations with GFP
434 were performed and embryos were analyzed for emigration of GFP^+ cells at E4. Images
435 presented are opposite a rostral somitic domain. Note the presence of emigrated RFP+ cells in
436 all treatments. Notice as well the presence of GFP^+ delaminated cells in F,F', while virtually
437 no GFP^+ cells are seen outside of the NT in E,E', G,G' and H,H'. (I) Quantification of
438 delaminated GFP^+ cells. Seventy sections per embryo were analyzed at an equivalent axial
439 level. N = 21, 19, 6 and 12 embryos were monitored for control, RARα403, Smad6 and
440 Smad6+RARα403 groups, respectively. *p < 0.05, ****p < 0.0001, approximate P-value
441 Kruskal-Wallis with post-hoc Dunn's test. Abbreviations, ns, not significant; NT, neural tube,
442 DRG, dorsal root ganglion. Scale bar, 50μm.

443

444

445 **Inhibition of RA signaling downregulates only a subset of RP markers**

446 A major question that remains to be addressed is whether the end of the NC stage is sufficient
447 for signaling the formation of the definitive RP, or whether these are two independently
448 regulated processes. Given that RA deficiency delays the end of the NC stage, we asked
449 whether this occurs at the expense of timely RP development.

450 As recently shown (Ofek et al., 2021), there are differences in the gene expression profile
451 between premigratory NC cells and definitive RP cells. We selected a number of RP-specific
452 genes that are not expressed in the dorsal NT during the NC stage and examined the effect of
453 RA downregulation on their expression. As described in Fig. 2, expression of RP-specific BMP
454 inhibitors was strongly reduced. Likewise, mRNA encoding *slit1*, a chemorepellent of post-
455 floor plate commissural axons (Kidd et al., 1999) was also decreased under experimental
456 conditions (Supplem. Fig. S5). In contrast, additional RP markers, such as *Rspo1, NDP (norrin)*
457 or *draxin*, were normally expressed (Supplem. Fig. S5), suggesting that development of a
458 number of RP traits is independent of RA signaling.

459 Since both NC and RP markers are present at the RP stage upon inhibition of RA signaling
460 (Figs.3, Supplem Fig. S5), we proceeded to clarify whether NC and RP markers are expressed
461 in the same cells, or, alternatively, whether there is a mix of different cell types in the RP of
462 RARα403-treated embryos. First, we performed ISH of *Rspo1* (RP marker) and *foxd3* (NC
463 marker) on adjacent sections of RP-stage embryos electroporated at E2.5 with either RARα403
464 or control GFP (Fig. 6). Whereas in control NTs, only *Rspo1* was apparent in the RP, both
465 *Rspo1* and *foxd3* were detected in an overlapping pattern in the RP of the treated embryos (Fig.
466 6A-B'''').

467 In addition, we combined a fluorescent ISH of *Rspo1* with immunostaining for SNAI2 or Sox9
468 in the same sections. Control NTs exhibited SNAI2 and Sox9^{+} nuclei only outside the *Rspo1*$^{+}$

469 RP (Fig.6C-C'', E-E", see also Fig. 3G-I). In striking contrast, both markers were detected in
470 the same dorsal NT cells in the absence of local RA signaling (Fig.6D-D", F-G", H,I). In some
471 instances, *Rspo1*$^{+}$Sox9^{+} cells were also noticed undergoing delamination from the NT (Fig.
472 6G-G", arrowhead).

473 Together, these data suggest that the loss of RA signaling does not totally prevent the advent
474 of RP markers implying that loss of NC identity and gain of RP fate are independently-
475 regulated processes. Nevertheless, timely RA activity in the dorsal NT is required for the proper
476 segregation of NC from RP fates.

477

Figure 6

Figure 6- Overlapping expression in RP of both NC and RP markers upon inhibition of RA signaling

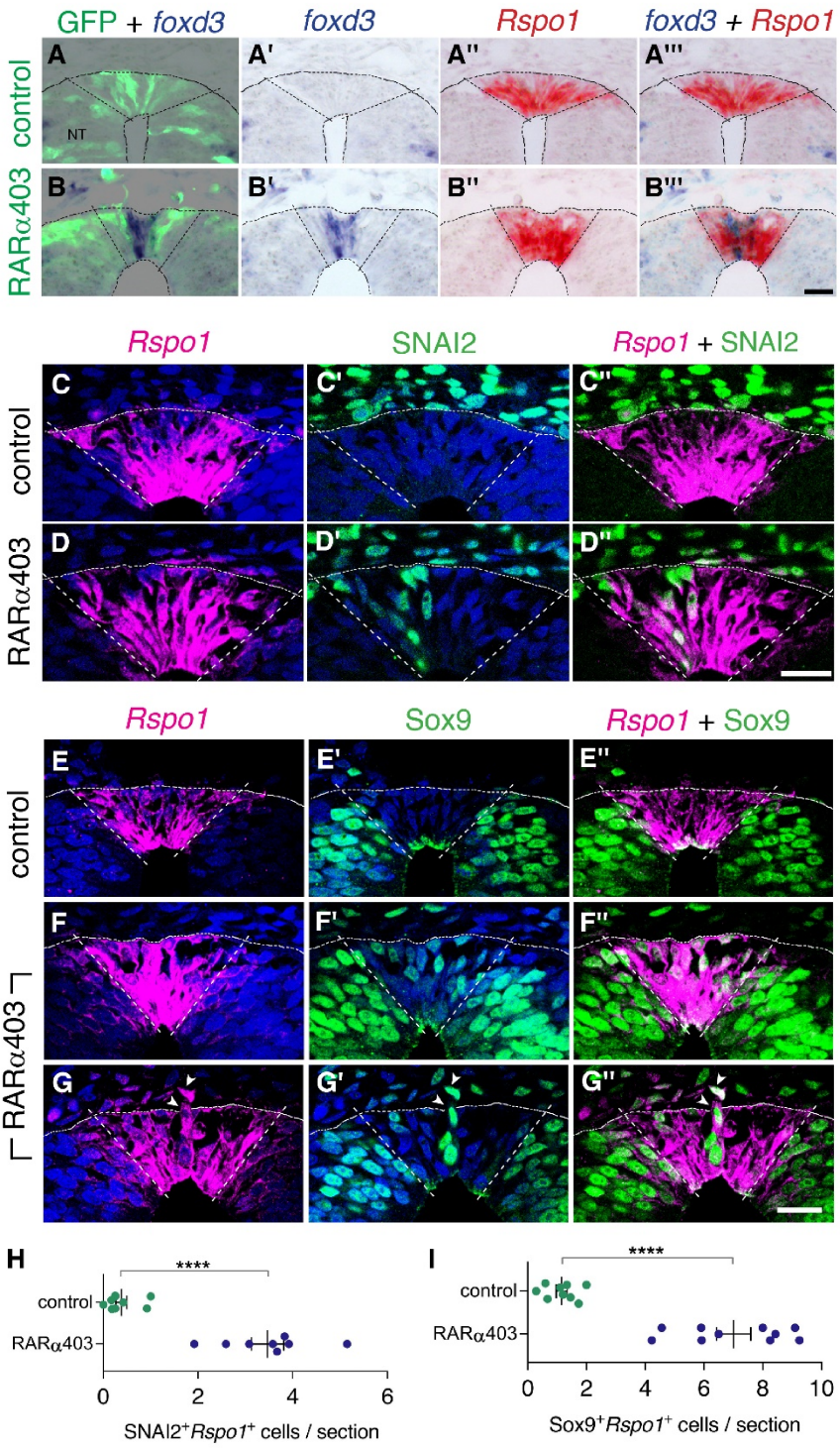

(A-B''') Embryos co-electroporated at E2.5 with either control PCAGG or RARα403 along with a GFP plasmid. Embryos were fixed at E4, and adjacent sections were in-situ hybridized for *foxd3* or *Rspo1* and then superimposed to reveal overlapping domains of gene expression. Dotted lines delineate the *Rspo1* expression domain. In control embryos, no *foxd3* expression was detected in the RP (N = 2, and see also Fig. 3). In RARα403-treated embryos, overlapping expression was detected in all 4 embryos examined.

(C-D") Immunostaining for SNAI2 and fluorescent ISH for *Rspo1* were combined on the same sections of embryos electroporated at E2.5 with either control PCAGG or RARα403 and analyzed at E4. Dashed lines mark the *Rspo1* expression domain. Note the presence of SNAI2$^+$*Rspo1*$^+$ cells in the RP in D". (E-G") Immunostaining for Sox9 and fluorescent ISH for *Rspo1* were performed as above. Note the presence of Sox9$^+$*Rspo1*$^+$ cells in the RP in F" and G''. Additionally, delaminating Sox9$^+$*Rspo1*$^+$ cells (arrowheads in G-G") were apparent under experimental conditions. (H,I) Quantification of SNAI2$^+$*Rspo1*$^+$ and Sox9$^+$*Rspo1*$^+$ cells in the RP. N = 8 and 8 for SNAI2 in controls and RARα403. N = 9 and 10 embryos for control and RARα403 groups stained with Sox9, respectively. ****$p < 0.0001$, Welch's t-test. Abbreviations, NT, neural tube. Scale bar, 20 µm.

519 **RP-derived dI1 interneuron development only partly depends on RA signaling**

520 We further investigated whether depletion of RA signaling had any effect on the role of the RP
521 as a signaling center for dorsal interneuron development. We immunostained RARα403 and
522 control-electroporated embryos with the dI1 interneuron marker BarHL1, and analyzed the
523 number of BarHL1$^+$ cells and their spatial distribution. Whereas no significant difference in
524 the number of BarHL1$^+$ interneurons could be monitored between control and treated embryos
525 (Fig. 7A), there was a collective dorsal shift in their position in the RARα403-treated NTs,
526 with some of BarHL1$^+$ cells residing in the RP domain itself (Fig. 7B-E', arrowheads).

527 Thus, whereas inhibition of RA signaling does not affect RP-mediated formation of dI1
528 interneurons, it interferes with the spatial information conveyed onto dorsal interneurons from
529 the RP, likely by impairing the formation of the boundary between the RP and more ventral
530 domains. These findings further indicate that RA signaling not necessarily influences
531 development of RP properties but rather impairs temporal and spatial segregation between
532 dorsal cell lineages.

Figure 7

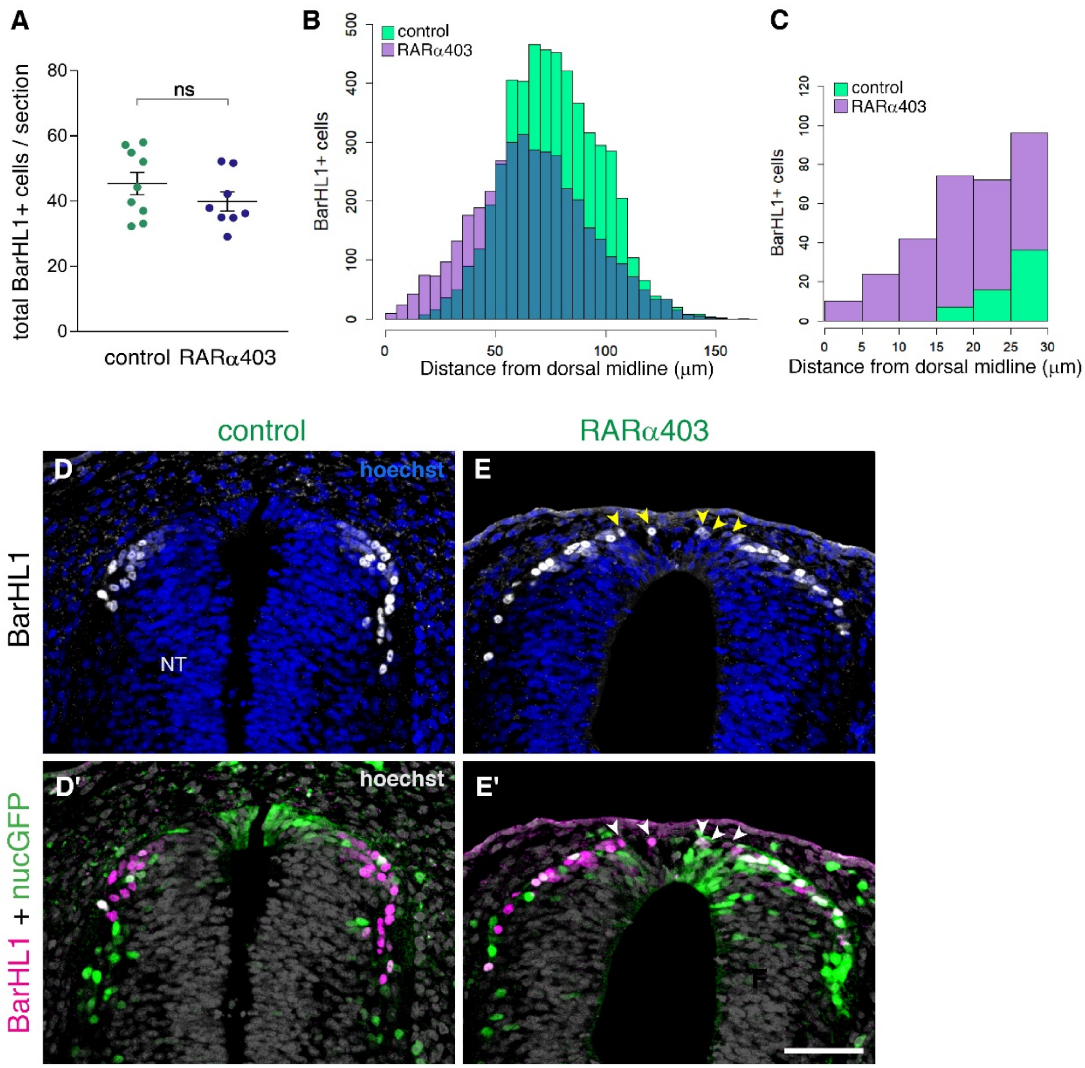

533

534 Figure 7- RP-derived dI1 interneuron development only partly depends on RA signaling

535 (A) Quantification of BarHL1^{+} dI1 interneurons in E4 embryos, electroporated at E2.5 with
536 either control PCAGG or RARα403. No significant difference in the number of BarHL1^{+}
537 neurons was monitored. Ten-to-14 sections were analyzed per embryo; N= 9 and 8 embryos
538 for control and RARα403 groups, respectively. Student's unpaired t-test was applied.

539 (B, C) Spatial distribution of BarHL1^{+} cells measured as the distance from the dorsal midline.
540 5126 cells were counted in the control group (green), and 3886 in the RARα403 group (purple).
541 The area of overlap of control and experimental cells is in blue. Note the dorsal shift of cells in
542 the RARα403-treated group when compared to controls. In (B) all the cells are included, while
543 in (C) only cells included in a 30 μm distance from the dorsal midline, comprising the RP
544 region, are presented.

545 (D-E') Confocal images of BarHL1-stained sections. Nuclear GFP (nucGFP) marks the
546 electroporated domain. Note in E and E' the presence of BarHL1^{+} interneurons inside the RP
547 domain (arrowheads) compared to controls in which these neurons are localized ventral to the
548 RP. Nuclei are visualized with Hoechst. Abbreviation, NT, neural tube. Scale bar, 50 μm.

549 **The dorsal NT as the source of RA responsible for NC to RP transition**

550 As shown in Fig. 1, the dorsal NT becomes a source of RA during the period marking the end
551 of NC emigration and transition to the RP stage, suggesting this is the local source of RA that
552 underlies the effects demonstrated here. Yet, at the same time, RA is still produced in the
553 adjacent paraxial mesoderm. To begin addressing whether the latter tissue accounts for the
554 effects observed, we separated the paraxial mesoderm from the NT with an impermeable
555 membrane and assessed the development of the RP. A unilateral slit was performed at the
556 epithelial somite stage into which a piece of aluminum foil was inserted (Fig. 8A). We analyzed
557 RP formation using *BAMBI* expression as a sensitive readout for normal RP ontogeny that is
558 downregulated in the absence of RA signaling (Fig.2). Notably, *BAMBI* remained strongly
559 expressed in the RP of treated embryos to the same extent as the control sides, despite
560 separation from the mesoderm and virtual disappearance of the somitic tissue that lost contact
561 with the NT (Fig. 8A-C'). To exclude the possibility that RA from the mesoderm of the non-
562 separated side is sufficient to induce normal RP development, a slit was made along the dorsal
563 midline of the NT following insertion of the barrier, thus opening the NT and creating a
564 physical gap between both halves of the neuroepithelium (Fig. 8D). A comparable expression
565 of *BAMBI* mRNA on both hemi-RPs was still apparent under these conditions (Fig.8E-F"),
566 suggesting that the paraxial mesoderm is not the source of RA important for NC to RP
567 transition.

Figure 8

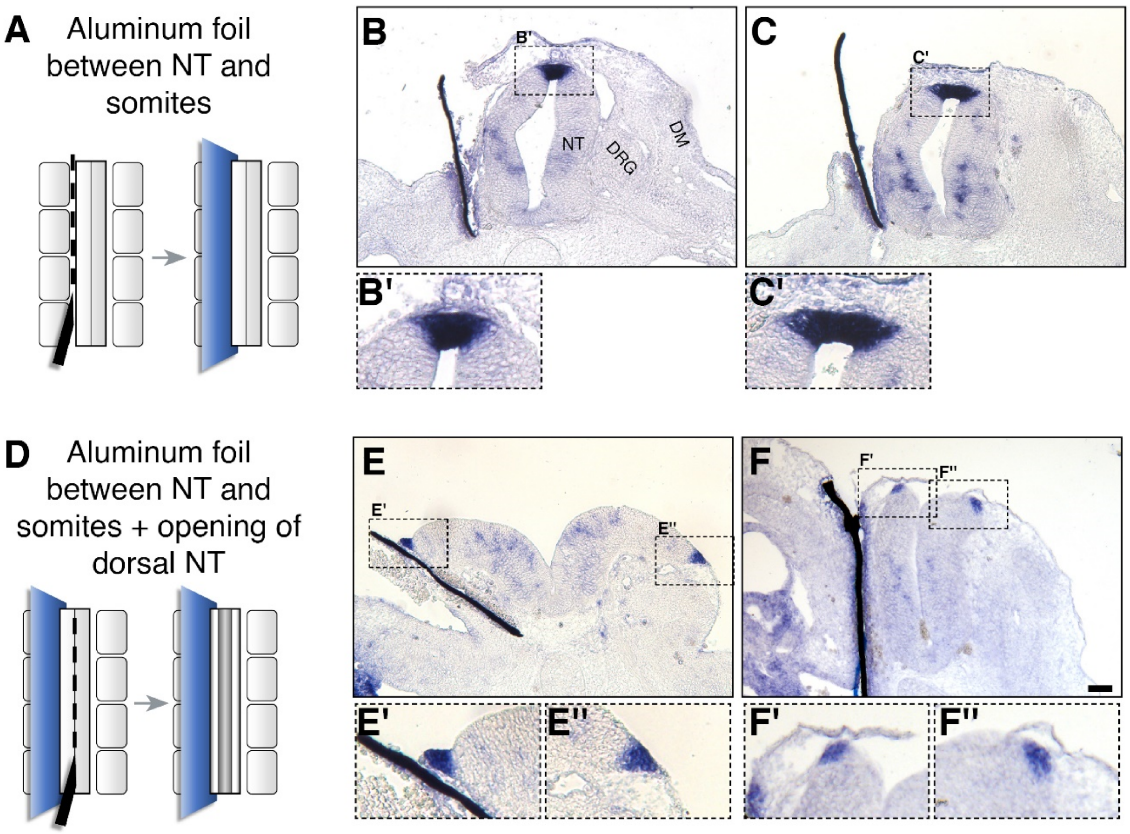

568

569 Figure 8- Somitic RA is dispensable for NC-to-RP transition

570 (A, D) Schematic representations of the experimental design to mechanically separate the NT
571 from somitic mesoderm using an impermeable aluminum foil (see Methods for details).

572 (B-C', E-F') ISH for *BAMBI* on sections of embryos with intact (B-C') or split (E-F") dorsal
573 NTs following grafting of a unilateral barrier between NT and somites. Representative images
574 from two different embryos are presented for each treatment. *BAMBI* expression remained
575 unchanged in the RP opposite to the operated sides in 7/7 embryos with an intact RP, and in
576 4/4 embryos with a split RP. Note as well that distal to the barriers, most of the somitic
577 mesoderm disappeared (B,C,E). In some instances, the somatic layer of the lateral plate
578 mesoderm approached the barrier (F). Abbreviations, DM, dermomyotome, DRG, dorsal root
579 ganglion, NT, neural tube. Scale bar, 50 μm.

580

Figure 9

Figure 9- Schematic diagram summarizing the role of RA in the transition from NC to RP

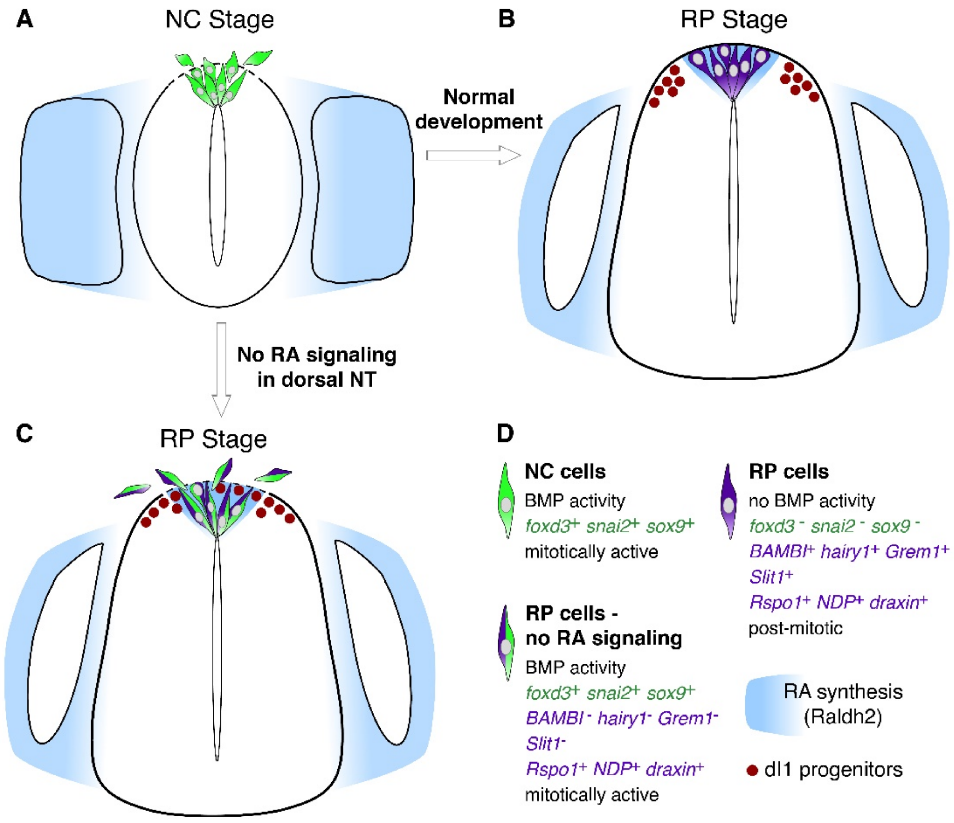

(A) At the NC stage, premigratory progenitors residing in the dorsal NT (green) exhibit BMP signaling activity, express specific NC markers (e.g. *foxd3*, *snai2* and *sox9*, green in D) and proliferate extensively. Following a process of EMT, NC cells delaminate from the NT through a discontinuous basement membrane (dashed line) to migrate away. At the NC stage, RA is supplied to the NT from the paraxial mesoderm, where it is produced by Raldh2 (blue).

(B) Under normal conditions, upon cessation of NC production and emigration, a definitive RP forms. RP cells (purple) are refractory to BMP signaling, and exhibit a different gene expression profile when compared to NC cells: they downregulate *foxd3*, *snai2* and *sox9* and upregulate RP-specific genes (purple in D), among which are known inhibitors of BMP signaling. RP cells gradually exit the cell cycle and do not delaminate, regenerating a continuous basement membrane and epithelial traits. During the transition between NC and RP stages, *Raldh2* expression begins in the dorsal NT (blue in RP), in addition to RA still produced in somites. The RP functions as a signaling center, regulating specification and/or differentiation of dorsal interneurons (red, dI1 progenitors) that localize ventral to the RP.

(C) In the present study we demonstrate that inhibition of RA signaling in the dorsal NT, impairs the end of NC production and consequently, the normal transition between NC and RP stages. First, under experimental conditions, dorsal NT cells at the RP stage retain active BMP signaling likely via downregulation of BMP antagonists (*BAMBI, hairy1, Grem1*) otherwise selectively expressed in RP. Second, they express both NC and RP markers (illustrated as green/purple cells), Third, they functionally behave as NC cells, maintaining mitotic activity, impaired epithelial traits (such as a discontinuous basement membrane, dashed line), and continuous emigration from the NT. Fourth, although the advent of several RP-specific markers is normal (e.g; *Rspo1, NDP, draxin*) and the number of dI1 progenitors is unchanged, the spatial segregation between NC, RP and dI1 interneuron lineages is compromised.

(D) A selection of differential traits displayed by NC progenitors (green), normal RP cells (purple), as well as of "RP" cells formed upon inhibition of RA signaling (green/purple). Selected NC genes appear in green and RP-specific genes in purple. (+) and (-) depict expression or lack of expression of relevant genes, respectively. Light blue color indicates sites of RA production (i.e. *Raldh2* expression). Red circles represent dI1 progenitors.

629 **Discussion**

630 Here we show that dorsal NT-derived RA controls the end of NC production and emigration
631 (Fig.9). This effect is mediated through BMP signaling, at least via the upregulation of BMP
632 inhibitors in the nascent RP, which prevent persistent BMP activity and ensures the timely
633 cessation of NC production (Fig.9). We previously reported that BMP produced in the dorsal
634 NT is an essential inducer of NC EMT and emigration; a graded activity of BMP is created
635 along the rostro-caudal axis of the embryo thanks to a counter-gradient of its inhibitor noggin.
636 By the time of initial somite dissociation, noggin expression is downregulated by somite
637 derived factors (Sela-Donenfeld and Kalcheim, 1999; Sela-Donenfeld and Kalcheim, 2002),
638 including an interplay between mesodermal RA and Fgf8, that affect the onset but not the
639 maintenance of NC delamination (Martínez-Morales et al., 2011). Our findings are consistent
640 with previous results reporting that RA repressed BMP signal in P19 embryonic carcinoma
641 cells; in vivo, RA antagonized BMP-regulated differentiation and proliferation of neural
642 progenitor cells in the NT (Sheng et al., 2010). Likewise, RA was also found to inhibit Wnt
643 signaling (Shaker et al., 2020), that in the present context acts downstream of BMP and whose
644 activity was enhanced by loss of RA signaling.

645 In normal development, the end of NC emigration is followed by the advent of the definitive
646 RP of the CNS (Rekler and Kalcheim, 2021). This is associated with a progressive withdrawal
647 from the cell cycle, the regeneration of a complete basal lamina overlying the dorsal NT, of
648 apico-basal properties of the RP epithelium and the corresponding downregulation and
649 upregulation, respectively, of NC and RP-specific genes (Nitzan et al., 2016; Ofek et al., 2021).
650 We report that, in the absence of RA activity, there is a continuity of several molecular and
651 cellular properties of the NC well into the RP stage, including the presence of a subset of RP

652 cells that co-expresses NC markers. Together, lack of local RA activity blurs the spatial and
653 temporal segregation between NC and RP (Fig.9).

654 Despite these phenotypes, it is notable that RP-specific markers such as *Rspo1*, *NDP* or *draxin*,
655 were not affected, suggesting that a RP is able to develop even if RA activity is inhibited. This
656 raises the fundamental question whether the end of NC formation and the ensuing development
657 of a RP are regulated by the same or by independent mechanisms. Our results would suggest
658 that the mechanisms accounting for the cessation of NC phase are necessary but not sufficient
659 to explain all aspects of RP development. Consistent with this notion, spatio-temporal lineage
660 tracings revealed that RP segregate from neural progenitors of the NC before the latter
661 complete emigration (Krispin et al., 2010b; Nitzan et al., 2012). In addition, gain and loss of
662 Notch function in avians and mice, respectively, resulted in changes in RP formation with no
663 apparent effects on NC cell behavior (Ofek et al., 2021). This would indicate that although NC
664 and RP lineages arise from common progenitors (Nitzan et al., 2012) by different exposure
665 times and/or levels of BMP signaling (Nitzan et al., 2016; Timmer et al., 2002; Tozer et al.,
666 2013), they segregate rather early from each other.

667 Among the RP genes whose expression is perturbed in the absence of RA signaling, we found
668 *BAMBI, hairy1* and *Gremlin*, none of which is expressed in the dorsal NT at NC stages. These
669 genes, whose transcription was prevented by treatment with RARα403 and/or Cyp26, encode
670 inhibitors of BMP signaling. Hence, RA-sensitive aspects of RP development are linked to its
671 regulation of BMP activity. Moreover, since RA-dependent downregulation of BMP activity
672 accounts for only selected facets of RP ontogeny, we posit that RP development comprises
673 both RA-dependent and RA-independent mechanisms.

674 We observed that maintenance of NC traits in RARα403-treated NTs did not interfere with
675 differentiation of a normal number of RP-dependent dorsal interneurons of type 1, suggesting

676 that the role of the RP as an interneuron inducer center was not altered. However, their
677 topographical dorsoventral distribution was abnormal as instead of organizing into discrete
678 nuclei, interneurons redistributed along the basal surface of the NT comprising the RP itself,
679 further demonstrating that the structural integrity of this signaling center and/or of its
680 boundaries is compromised; this is consistent with the observed local changes in epithelial
681 architecture, cell cycle properties and basal lamina deposition.

682 Since dI1 interneurons are also specified by BMP signaling (Chesnutt et al., 2004; Hegarty et
683 al., 2013; Timmer et al., 2002), it is conceivable to speculate that maintenance of BMP
684 responsiveness in the RP of RARα403-treated NTs affects the normal dorso-ventral gradient
685 of BMP activity (Tozer et al., 2013), perhaps eliciting indirectly an attractive function that
686 enables dI1 interneurons to migrate into the RP domain. In this context, RP-derived BMP
687 exhibits at a later stage chemorepellent properties vis-à-vis commissural axons (Augsburger et
688 al., 1999; Butler and Dodd, 2003), putting forward the additional possibility of guidance
689 functions for this morphogen under the present experimental conditions. One of the genes
690 downregulated upon abrogation of RA function is *Slit1*, a known repellent of axonal guidance
691 (Kidd et al., 1999), as well as of cell migration (Halperin-Barlev and Kalcheim, 2011;
692 Theveneau and Mayor, 2012). Loss of *Slit1* could also account for the dorsal shift of dI1
693 interneurons into the RP domain, and possible interactions with BMP remain to be examined,

694 It is worth mentioning that the NT is sensitive to RA throughout development, with RA playing
695 various functions at different stages [this study, (Diez del Corral and Morales, 2014; Martinez-
696 Morales et al., 2011; Wilson et al., 2004)]. Hence, it is plausible that the mechanisms mediating
697 these effects differ as a function of time and context. Here we report that precisely before the
698 end of NC delamination, RA begins to be synthesized in the dorsal NT (e.g; *Raldh2* expression)
699 in addition to the paraxial mesoderm, raising the notion that this new, local source of RA

700 accounts for the end of NC development. Notably, *Raldh2* is also synthesized in the RP of
701 mouse embryos (Ofek et al., 2021). Unfortunately, available mutants of *Raldh2* are embryonic
702 lethal at about E8.75 (Niederreither et al., 1999), precluding a focal analysis of the transition
703 from NC to RP. In this sense, the avian embryo provides an excellent model to address events
704 restricted both in time and space. The two methods we implemented to abrogate RA signaling
705 in the dorsal NT act primarily in a cell autonomous fashion. However, it is still possible that
706 given the secreted nature of the ligand, Cyp26A1 and/or RARα403 missexpression in the
707 dorsal NT also provide a sink for somitic RA. Despite robust separation of the mesoderm from
708 the NT, expression of *BAMBI*, a most sensitive and significant readout of RA activity, was not
709 altered, suggesting that mesodermal RA is dispensable. What accounts for this shift in
710 responsiveness from a mesodermal towards a neural source of factor? First, local RA could
711 provide a stronger and more efficient signal to target progenitors given the increasing size of
712 the embryo and the development of a continuous basement membrane dorsal to the NT.
713 Second, cofactors of RA such as *Crabp1*, could change the nature of the cellular response upon
714 late appearance at the RP stage. Together, changes in the molecular landscape between NC and
715 RP stages (Ofek et al., 2021), that partly depend on local RA activity, may alter the nature of
716 the interactions between RA and BMP/Wnt to signal a timely cessation of NC production.
717 Along this line, the present study provides a mechanistic explanation for the separation between
718 PNS (NC) and CNS (RP and dI1) lineages during development.

719

720 **Materials and Methods**

721 Embryos

722 Fertilized quail (*Coturnix coturnix Japonica*) eggs were obtained from commercial sources
723 (Moshav Mata), kept at 15°C and then incubated at 38 °C to desired stages. Embryos were
724 staged by the number of somite pairs formed. All experiments were conducted at the flank level
725 of the axis.

726

727 Expression vectors and *in ovo* electroporation

728 The following expression vectors were used as controls: pCAGG, pCAGGS-EGFP (Krispin et
729 al., 2010b), pCAG-mGFP (Addgene #14757), pCAGGS-RFP (Ofek et al., 2021). PCAGGS-
730 RARα403 and PCAGGS-Cyp26A1 (subcloned from PCAGGS-RARα403-IRES-eGFP and
731 PCAGGS-Cyp26A1-IRES-eGFP, respectively, from S. Sockanathan (Novitch et al.,
732 2003), were applied to inhibit RA activity. pCAB-cSmad6 was implemented to inhibit BMP
733 activity (Nitzan et al., 2016).

734 To monitor RA activity, we used the pGL3-RARE-SV40-AP reporter [from J. Sen, (Gupta and
735 Sen, 2015)]. Fluorescent versions of this reporter were prepared by replacing the AP tag with
736 either RFP or with a destabilized version of GFP (pGL3-RARE-SV40-RFP and pGL3-RARE-
737 SV40-d2EGFP, respectively (Clontech). Wnt activity was measured with 12XTOPFLASH-
738 d2EGFP (Rios et al., 2010).

739 Unilateral, bilateral and/or double electroporations to the NT were performed as detailed under
740 Results. To this end, DNA (4 ug/ul) was mixed with Fast Green and microinjected into the
741 lumen of the NT at the flank level of the axis. Five mm tungsten electrodes were placed on

742 either side of the embryo. A square wave electroporator (BTX, San Diego, CA, USA) was used
743 to deliver one pulse of current at 17–25 V for 6 ms.

744

745 Mechanical separation of the paraxial mesoderm from the NT

746 A unilateral slit between epithelial somites and NT comprising an approximate length of 8
747 segments was performed. A piece of aluminum foil was then inserted that extended beyond the
748 dorsal border of the tissues to provide a continuous barrier despite embryo growth. In some
749 cases, the dorsal NT was additionally opened to separate between both halves of the
750 neuroepithelium. Following microsurgery, embryos were reincubated for 48 hours prior to
751 fixation.

752

753 Immunohistochemistry

754 For immunostaining, embryos were fixed overnight at 4 °C with 4% formaldehyde (PFA) in
755 phosphate-buffered saline (PBS) (pH 7.4), embedded in paraffin wax and serially sectioned at
756 8 μm. Immunostaining was performed either on whole mount embryos or on paraffin sections,
757 as previously described (Burstyn-Cohen and Kalcheim, 2002; Kahane and Kalcheim, 2020).
758 Antibodies were diluted in PBS containing 5% fetal bovine serum (Biological Industries Israel,
759 04-007-1A) and 1% or 0.1% Triton X-100 (Sigma Aldrich Israel, X-100), respectively.
760 Antibodies used were: rabbit anti-GFP (1:1000, Invitrogen, Thermo-Fisher Scientific, A-
761 6455), mouse anti-GFP (1:100, Abcam, Ab38689), rabbit anti-RFP (1:1000, OriGene,
762 AP09229PU-N), guinea pig anti-pSmad1/5/8 (1:300, a gift from E. Laufer), mouse anti-H3-
763 pS10 (1:400, Abcam, Ab14955), rabbit anti-Laminin (1:100, Sigma Israel, L9393), rabbit anti-
764 Sox9 (1:150, Millipore, AB5535), rabbit anti-SNAI2 (1:500; Cell Signaling Technologies,

765 9585), mouse anti-CD57 (anti-HNK1, 1:500, BD Biosciences, 559048), rabbit anti-BarHL1
766 (1:300, Sigma Israel, HPA004809). Cell nuclei were visualized with 125 ng/ml Hoechst 33258
767 (Sigma Israel, 14530) diluted in PBS.

768

769 In-situ hybridization

770 For *in-situ* hybridization (ISH), embryos were fixed with Fornoy (60% ethanol, 30%
771 formaldehyde and 10% acetic acid) for 1 hour at room temperature, embedded in paraffin wax
772 and serially sectioned at 10 μm. ISH was performed on sections. In brief, sections were treated
773 with 1 ug/ml proteinase K, refixed in 4% PFA, then hybridized overnight at 65 °C with
774 digoxigenin-labeled RNA probes (Roche, 11277073910). The probes were detected with AP
775 coupled with anti-digoxigenin Fab fragments (Roche, 11093274910). AP reaction was
776 developed with 4-Nitro blue tetrazolium chloride (NBT, Roche, 11383213001) and 5-bromo-
777 4-chloro-3'-indolyphosphate p-toluidine salt (BCIP, Sigma Israel, B8503). In the *foxd3/Rspo1*
778 ISH experiment, the AP reaction of *Rspo1* was developed with Fast Red (Sigma Israel, F4648)
779 for 2 hours at room temperature. Importantly, all hybridizations, whether done on intact
780 embryos at NC vs. RP stages, or in control vs. experimental embryos, were always developed
781 for the same time per given probe and experiment. The RNA probes used are described in Table
782 S1. Several probes were produced by PCR amplification (KAPA2G Fast ReadyMix PCR kit,
783 Sigma Israel, KK5101). cDNA templates were synthesized by RNA precipitation followed by
784 reverse transcription PCR. RNAs were produced from 20ss-E4 quail embryos. Tissue samples
785 were homogenized with TriFast reagent, and RNA was separated with chloroform and
786 isopropanol. The primers used are depicted in Table S1.

787

788 Data acquisition and statistical analysis

789 *Measurement of the intensity of immunofluorescence and ISH signals:* Intensities were
790 measured using FIJI (Schindelin et al., 2009). In most cases, the RP was selected as the region
791 of interest (ROI); mean intensity was measured and background intensity was then subtracted.
792 Average intensity of all sections was calculated per embryo, and values were normalized with
793 a control mean set as 1.

794 For measurement of phospho-Smad1/5/8 intensity, the ROI was selected as the dorsal domain
795 of the NT from the dorsal midline to the ventral border of dI1 progenitors.

796 To monitor intensity of laminin immunostaining in the RP basal lamina, a segmented line of
797 width 4 was drawn along the basal aspect of the RP, and mean intensity was measured within
798 that area. Average intensity was calculated for each embryo and expressed relative to a control
799 value set as 1.

800 To measure the relative position of cell nuclei across the apico-basal extent of the RP, the latter
801 was divided into basal and apical halves, and Hoechst-stained nuclei were manually counted
802 in both domains.

803 The distance of BarHL1^{+} cells from the dorsal midline of the NT was measured for each cell
804 manually using FIJI, and histograms were generated using R (https://www.R-project.org/) in
805 Rstudio (http://www.rstudio.com/).

806 Images were photographed using a DP73 (Olympus) cooled CCD digital camera mounted on
807 a BX51 microscope (Olympus) with Uplan FL-N 20x/0.5 and 40x/0.75 dry objectives
808 (Olympus). Confocal sections encompassing their entire thickness were photographed using a
809 Nikon Eclipse 90i microscope with a Plan Apo 40x/1.3 or 100x/1.4 objectives (Nikon) and a

810 D-Eclipse c1 confocal system (Nikon) at 1.0 μm increments through the z-axis. Images were
811 z-stacked with FIJI software.

812 For quantification, images of control and treated sections were photographed under the same
813 conditions. For figure preparation, images were exported into Photoshop CS6 (Adobe). If
814 necessary, the levels of brightness and contrast were adjusted to the entire image and images
815 were cropped without color correction adjustments or γ adjustments. Graphics were generated
816 using Graphpad Prism 7.0, and figures were prepared using Photoshop and InDesign CS6.

817 Results were processed with Graphpad Prism 7 and presented as scatter plots with mean±SEM.
818 Data were subjected to statistical analysis using either of the following tests, as described in
819 the respective legends to Figures: Student's t-test, Welch's t-test, Mann-Whitney test, 1-way
820 ANOVA with post-hoc Tukey test, Kruskal-Wallis with post-hoc Dunn's test and Wilcoxon
821 signed ranks test. All tests applied were two-tailed and a P-value ≤ 0.05 was considered
822 significant.

823

824 **Acknowledgments**

825 We are grateful to all the researchers whose names are mentioned along the text for generously
826 providing reagents. We thank Avihu Klar and Joel Yisraeli for critical reading of the
827 manuscript. This study was supported by grants from the Israel Science Foundation (ISF
828 #209/18) and from the Ines Mandl Research Fund (IMRF) to CK.

829 **Author Contributions**

830 DR and CK conceived the article, wrote it and prepared the Figures. DR performed the
831 experiments. Both authors discussed and agreed on the text and approved the manuscript.

Conflicts of Interest

The authors declare no conflict of interests

835 **References**

836 **Andrews, M. G., Kong, J., Novitch, B. G. and Butler, S. J.** (2019). New perspectives on
837 the mechanisms establishing the dorsal-ventral axis of the spinal cord. *Curr Top Dev*
838 *Biol* **132**, 417–450.

839 **Augsburger, A., Schuchardt, A., Hoskins, S., Dodd, J. and Butler, S.** (1999). Bmps as
840 mediators of roof plate repulsion of commissural neurons. *Neuron* **24**, 127–141.

841 **Berggren, K., McCaffery, P., Drager, U. and Forehand, C. J.** (1999). Differential
842 distribution of retinoic acid synthesis in the chicken embryo as determined by
843 immunolocalization of the retinoic acid synthetic enzyme, RALDH-2. *Dev Biol* **210**,
844 288–304.

845 **Blentic, A., Gale, E. and Maden, M.** (2003). Retinoic acid signalling centres in the avian
846 embryo identified by sites of expression of synthesising and catabolising enzymes. *Dev*
847 *Dyn* **227**, 114–127.

848 **Brazil, D. P., Church, R. H., Surae, S., Godson, C. and Martin, F.** (2015). BMP
849 signalling: agony and antagony in the family. *Trends Cell Biol* **25**, 249–264.

850 **Burstyn-Cohen, T. and Kalcheim, C.** (2002). Association between the cell cycle and neural
851 crest delamination through specific regulation of G1/S transition. *Dev. Cell* **3**,.

852 **Burstyn-Cohen, T., Stanleigh, J., Sela-Donenfeld, D. and Kalcheim, C.** (2004). Canonical
853 Wnt activity regulates trunk neural crest delamination linking BMP/noggin signaling
854 with G1/S transition. *Development* **131**, 5327–5339.

855 **Butler, S. J. and Dodd, J.** (2003). A role for BMP heterodimers in roof plate-mediated
856 repulsion of commissural axons. *Neuron* **38**, 389–401.

857 **Chambers, D., Wilson, L., Maden, M. and Lumsden, A.** (2007). RALDH-independent

858 generation of retinoic acid during vertebrate embryogenesis by CYP1B1. *Development*
859 **134**, 1369–1383.

860 **Chesnutt, C., Burrus, L. W., Brown, A. M. and Niswander, L.** (2004). Coordinate
861 regulation of neural tube patterning and proliferation by TGFbeta and WNT activity.
862 *Dev Biol* **274**, 334–347.

863 **Chizhikov, V. V and Millen, K. J.** (2005). Roof plate-dependent patterning of the vertebrate
864 dorsal central nervous system. *Dev Biol* **277**, 287–295.

865 **Diez del Corral, R. and Morales, A. V.** (2014). Retinoic acid signaling during early spinal
866 cord development. *J. Dev. Biol.* **2**, 174–197.

867 **Diez del Corral, R., Olivera-Martinez, I., Goriely, A., Gale, E., Maden, M. and Storey,**
868 **K.** (2003). Opposing FGF and retinoid pathways control ventral neural pattern, neuronal
869 differentiation, and segmentation during body axis extension. *Neuron* **40**, 65–79.

870 **Duval, N., Vaslin, C., Barata, T. C., Frarma, Y., Contremoulins, V., Baudin, X.,**
871 **Nedelec, S. and Ribes, V. C.** (2019). BMP4 patterns Smad activity and generates
872 stereotyped cell fate organization in spinal organoids. *Development* **146**, doi:
873 10.1242/dev.175430.

874 **Endo Y., Osumi N. and Wakamatsu Y.** (2003). Bimodal functions of Notch-mediated
875 signaling are involved in neural crest formation during avian ectoderm development.
876 *Development.* **129**, 863–873.

877 **George, L., Chaverra, M., Todd, V., Lansford, R. and Lefcort, F.** (2007). Nociceptive
878 sensory neurons derive from contralaterally migrating, fate-restricted neural crest cells.
879 *Nat Neurosci* **10**, 1287–1293.

880 **Gupta, S. and Sen, J.** (2015). Retinoic acid signaling regulates development of the dorsal

881 forebrain midline and the choroid plexus in the chick. *Dev.* **142**, 1293–1298.

882 **Halperin-Barlev, O. and Kalcheim, C.** (2011). Sclerotome-derived slit1 drives directional
883 migration and differentiation of robo2-expressing pioneer myoblasts. *Development* **138**,.

884 **Haselbeck, R. J., Hoffmann, I. and Duester, G.** (1999). Distinct functions for Aldh1 and
885 Raldh2 in the control of ligand production for embryonic retinoid signaling pathways.
886 *Dev. Genet.* **25**, 353–364.

887 **Hegarty, S. V., O'Keeffe, G. W. and Sullivan, A. M.** (2013). BMP-Smad 1/5/8 signalling
888 in the development of the nervous system. *Prog. Neurobiol.* **109**, 28–41.

889 **Kahane, N. and Kalcheim, C.** (1998). Identification of early postmitotic cells in distinct
890 embryonic sites and their possible roles in morphogenesis. *Cell Tissue Res.* **294**, 297–
891 307.

892 **Kahane, N. and Kalcheim, C.** (2020). Neural tube development depends on notochord-
893 derived sonic hedgehog released into the sclerotome. *Development* **147**,.

894 **Kalcheim, C.** (2018). Neural crest emigration: From start to stop. *Genesis* **56**,.

895 **Kalcheim, C. and Kumar, D.** (2017). Cell fate decisions during neural crest ontogeny. *Int. J.*
896 *Dev. Biol.* **61**, 195–203.

897 **Kam, R. K. T., Deng, Y., Chen, Y. and Zhao, H.** (2012). Retinoic acid synthesis and
898 functions in early embryonic development. *Cell Biosci.* **2**, 11.

899 **Kidd, T., Bland, K. S. and Goodman, C. S.** (1999). Slit is the midline repellent for the robo
900 receptor in Drosophila. *Cell* **96**, 785–794.

901 **Krispin, S., Nitzan, E. and Kalcheim, C.** (2010a). The dorsal neural tube: A dynamic
902 setting for cell fate decisions. *Dev. Neurobiol.* **70**,.

903 **Krispin, S., Nitzan, E., Kassem, Y. and Kalcheim, C.** (2010b). Evidence for a dynamic
904 spatiotemporal fate map and early fate restrictions of premigratory avian neural crest.
905 *Development* **137**, 585–595.

906 **Kukreja, S., Udaykumar, N., Yogesh, B. and Sen, J.** (2020). Retinoic acid signaling
907 regulates proliferation and lamina formation in the developing chick optic tectum. *Dev.*
908 *Biol.* **467**, 95–107.

909 **Lara-Ramírez, R., Zieger, E. and Schubert, M.** (2013). Retinoic acid signaling in spinal
910 cord development. *Int. J. Biochem. Cell Biol.* **45**, 1302–1313.

911 **Le Douarin, N. M. and Kalcheim, C.** (1999). *The Neural Crest*. 2nd ed. New York:
912 Cambridge University Press.

913 **Le Dréau, G. and Martí, E.** (2013). The multiple activities of BMPs during spinal cord
914 development. *Cell. Mol. Life Sci.* **70**, 4293–4305.

915 **Lee, K. J., Mendelsohn, M. and Jessell, T. M.** (1998). Neuronal patterning by BMPs: a
916 requirement for GDF7 in the generation of a discrete class of commissural interneurons
917 in the mouse spinal cord. *Genes Dev.* **12**, 3394–3407.

918 **Maden, M., Ong, D. E., Summerbell, D., Chytil, F. and Hirst, E. A.** (1989). Cellular
919 retinoic acid-binding protein and the role of retinoic acid in the development of the chick
920 embryo. *Dev. Biol.* **135**, 124–132.

921 **Martinez-Morales, P. L., Diez del Corral, R., Olivera-Martinez, I., Quiroga, A. C., Das,**
922 **R. M., Barbas, J. A., Storey, K. G. and Morales, A. V** (2011). FGF and retinoic acid
923 activity gradients control the timing of neural crest cell emigration in the trunk. *J Cell*
924 *Biol* **194**, 489–503.

925 **Martínez-Morales, P. L., del Corral, R. D., Olivera-Martínez, I., Quiroga, A. C., Das, R.**

926 **M., Barbas, J. A., Storey, K. G. and Morales, A. V.** (2011). FGF and retinoic acid
927 activity gradients control the timing of neural crest cell emigration in the trunk. *J. Cell*
928 *Biol.* **194**, 489–503.

929 **Muroyama, Y., Fujihara, M., Ikeya, M., Kondoh, H. and Takada, S.** (2002). Wnt
930 signaling plays an essential role in neuronal specification of the dorsal spinal cord.
931 *Genes Dev.* **16**, 548–553.

932 **Niederreither, K., Subbarayan, V., Dollé, P. and Chambon, P.** (1999). Embryonic retinoic
933 acid synthesis is essential for early mouse post- implantation development. *Nat. Genet.*
934 **21**, 444–448.

935 **Nieto, M. A., Sargent, M. G., Wilkinson, D. G. and Cooke, J.** (1994). Control of cell
936 behavior during vertebrate development by slug, a zinc finger gene. *Science (80-.).* **264**,
937 835–839.

938 **Nitzan, E., Krispin, S., Pfaltzgraff, E. R., Klar, A., Labosky, P. A. and Kalcheim, C.**
939 (2012). A dynamic code of dorsal neural tube genes regulates the segregation between
940 neurogenic and melanogenic neural crest cells. *Dev.* **140**,.

941 **Nitzan, E., Avraham, O., Kahane, N., Ofek, S., Kumar, D. and Kalcheim, C.** (2016).
942 Dynamics of BMP and Hes1/Hairy1 signaling in the dorsal neural tube underlies the
943 transition from neural crest to definitive roof plate. *BMC Biol.* **14**, 23. DOI
944 10.1186/s12915-016-0245–6.

945 **Novitch, B. G., Wichterle, H., Jessell, T. M. and Sockanathan, S.** (2003). A requirement
946 for retinoic acid-mediated transcriptional activation in ventral neural patterning and
947 motor neuron specification. *Neuron* **40**, 81–95.

948 **Ofek, S., Wiszniak, S., Kagan, S., Tondl, M., Schwarz, Q. and Kalcheim, C.** (2021).

949 Notch signaling is a critical initiator of roof plate formation as revealed by the use of
950 RNA profiling of the dorsal neural tube. *BMC Biol.* **19:84**,
951 https://doi.org/10.1186/s12915-021-01014-3.

952 **Reijntjes, S., Blentic, A., Gale, E. and Maden, M.** (2005). The control of morphogen
953 signalling: regulation of the synthesis and catabolism of retinoic acid in the developing
954 embryo. *Dev Biol* **285**, 224–237.

955 **Rekler, D. and Kalcheim, C.** (2021). From Neural Crest to Definitive Roof Plate : The
956 Dynamic Behavior of the Dorsal Neural Tube. *Int. J. Mol. Sci.* **22**, 3911.

957 **Rhinn, M. and Dollé, P.** (2012). Retinoic acid signalling during development. *Development*
958 **139**, 843–858.

959 **Rios, A. C., Denans, N. and Marcelle, C.** (2010). Real-time observation of Wnt beta-catenin
960 signaling in the chick embryo. *Dev Dyn* **239**, 346–353.

961 **Schindelin, J., Arganda-Carrera, I., Frise, E., Verena, K., Mark, L., Tobias, P., Stephan,**
962 **P., Curtis, R., Stephan, S., Benjamin, S., et al.** (2009). Fiji - an Open platform for
963 biological image analysis. *Nat. Methods* **9**,.

964 **Sela-Donenfeld, D. and Kalcheim, C.** (1999). Regulation of the onset of neural crest
965 migration by coordinated activity of BMP4 and Noggin in the dorsal neural tube.
966 *Development* **126**, 4749–4762.

967 **Sela-Donenfeld, D. and Kalcheim, C.** (2002). Localized BMP4-noggin interactions generate
968 the dynamic patterning of noggin expression in somites. *Dev. Biol.* **246**,.

969 **Shaker, M. R., Lee, J., Park, S., Kim, J. Y., Son, G. H., Son, J. W., Park, B. H., Rhyu, I.**
970 **J., Kim, H. and Sun, W.** (2020). Stem Cell Reports. *Stem Cell Reports* **15**, 1–14.

971 **Sheng, N., Xie, Z., Wang, C., Bai, G., Zhang, K., Zhu, Q., Song, J., Guillemot, F., Chen,**

Y. G., Lin, A., et al. (2010). Retinoic acid regulates bone morphogenic protein signal duration by promoting the degradation of phosphorylated Smad1. *Proc. Natl. Acad. Sci. U. S. A.* **107**, 18886–18891.

Shinozuka, T., Takada, R., Yoshida, S., Yonemura, S. and Takada, S. (2019). Wnt produced by stretched roof-plate cells is required for the promotion of cell proliferation around the central canal of the spinal cord. *Development* **146**,.

Sun, J., Zhuang, F. F., Mullersman, J. E., Chen, H., Robertson, E. J., Warburton, D., Liu, Y. H. and Shi, W. (2006). BMP4 activation and secretion are negatively regulated by an intracellular Gremlin-BMP4 interaction. *J. Biol. Chem.* **281**, 29349–29356.

Theveneau, E. and Mayor, R. (2012). Neural crest migration: interplay between chemorepellents, chemoattractants, contact inhibition, epithelial-mesenchymal transition, and collective cell migration. *Wiley Interdiscip Rev Dev Biol* **1**, 435–445.

Timmer, J. R., Wang, C. and Niswander, L. (2002). BMP signaling patterns the dorsal and intermediate neural tube via regulation of homeobox and helix-loop-helix transcription factors. *Development* **129**, 2459–2472.

Tozer, S., Le Dreau, G., Marti, E. and Briscoe, J. (2013). Temporal control of BMP signalling determines neuronal subtype identity in the dorsal neural tube. *Development* **140**, 1467–1474.

Venepally, P., Reddy, L. G. and Sani, B. P. (1996). Characterization of cellular retinoic acid-binding protein I from chick embryo and its ligand binding properties. *Arch.Biochem.Biophys.* **336**, 231–239.

Wilson, L., Gale, E., Chambers, D. and Maden, M. (2004). Retinoic acid and the control of dorsoventral patterning in the avian spinal cord. *Dev Biol* **269**, 433–446.

995 **Wine-Lee, L., Ahn, K. J., Richardson, R. D., Mishina, Y., Lyons, K. M. and Crenshaw,**
996 **E. B.** (2004). Signaling through BMP type 1 receptors is required for development of
997 interneuron cell types in the dorsal spinal cord. *Development* **131**, 5393–5403.

998 **Xing, L., Anbarchian, T., Tsai, J. M., Plant, G. W. and Nusse, R.** (2018). Wnt/beta-
999 catenin signaling regulates ependymal cell development and adult homeostasis. *Proc*
1000 *Natl Acad Sci U S A* **115**, E5954–E5962.

1001 **Zechner, D., Muller, T., Wende, H., Walther, I., Taketo, M. M., Crenshaw 3rd, E. B.,**
1002 **Treier, M., Birchmeier, W. and Birchmeier, C.** (2007). Bmp and Wnt/beta-catenin
1003 signals control expression of the transcription factor Olig3 and the specification of spinal
1004 cord neurons. *Dev Biol* **303**, 181–190.

1005